

TOPOLOGICAL QUANTUM TELEPORTATION AND SUPERDENSE CODING WITHOUT BRAIDING

SACHIN J. VALERA [†]

ABSTRACT. We present the quantum teleportation and superdense coding protocols in the context of topological qudits, as realised by anyons. The simplicity of our proposed realisation hinges on the monoidal structure of Tambara-Yamagami categories, which readily allows for the generation of maximally entangled qudits. In particular, we show that both protocols can be performed without any braiding of anyons. Our exposition makes use of the graphical calculus for braided fusion categories, a medium in which the protocols find a natural interpretation. We also find a braid-free realisation of the Pauli gates using Ising anyons.

CONTENTS

1. Introduction	1
2. Review of Algebraic Theory of Anyons	5
3. Teleportation of Qubits by Braiding Ising Anyons	11
4. Superdense Coding of Bits by Braiding Ising Anyons	20
5. Qudit Teleportation and d -ary Superdense Coding Without Braiding	22
References	30

1. INTRODUCTION

1.1. Motivation. Anyons are localised quasiparticles, expected to arise in $(2+1)$ -dimensional condensed matter systems. When the Hilbert space of two or more anyons has dimension $d > 1$, at least one of the constituent anyons is said to be *nonabelian*; else, they are all called *abelian*. A sequence of particle exchanges (henceforth referred to as *braiding*)¹ should realise the action of a $U(d)$ -operator on their Hilbert space. The ability to control systems hosting nonabelian anyons holds particular allure, as it would amount to manipulating (topologically protected) qudits.²

It is predicted that anyons should manifest in a variety of settings. One of the most pursued directions is via the fractional quantum Hall effect, whose low-energy excitations were argued by Moore & Read (1991) to be anyons [1]. To date, it appears that the only widely accepted evidence of anyons comes from the $\nu = 1/3$ filling of the fractional quantum Hall effect, where Nakamura et al. and Bartolomei et al. (2020) observed signatures of *abelian* anyons [2, 3].

In the nonabelian case, perhaps the most promising candidate for near-term realisation is the *Ising* anyon (see for instance, the experiments of Willett et al. (2023) which probe $\nu = 5/2, 7/2$ [4]). A different, considerably popular approach of note has been *Majorana zero modes* (MZMs): these are quasiparticles trapped at the end of 1-dimensional wires, which to some extent, coincide with Ising anyons.³ At present, experimental evidence for Ising anyons and MZMs alike, remains inconclusive.⁴ From this doubt, an interesting line of thought has emerged: that *the realisation and manipulation of a topological qudit would credibly demonstrate the existence of nonabelian anyons*.⁵

[†]Center for Quantum and Topological Systems, New York University Abu Dhabi.

¹Viewed in $(2+1)$ -dimensions, exchanging anyons amounts to braiding their worldlines.

²A *qudit* is the d -ary generalisation of a qubit (i.e. a quantum state in a d -dimensional space).

³Indeed, MZMs have the same fusion rules as Ising anyons, and are protected by an energy gap. Unlike anyons, MZMs are quasiparticles in $(1+1)$ -d systems; nonetheless, schemes have been proposed for realising nonabelian braiding statistics of MZMs by setting up networks of wires. E.g. adjacent modes (with a T-junction in-between) can be exchanged by intermediately moving one mode into the junction. The orientation of the exchange is determined by which mode is placed in the junction.

⁴The quest for MZMs in particular, has recently experienced some setbacks [5, 6].

⁵For instance, see [7, 28:45-29:10].

1.2. Approach. With the above in mind, we set about the task of designing simple quantum protocols using nonabelian anyons; namely, *teleportation* and its dual protocol, *superdense coding*.

Both protocols rely on the presence of a *maximally entangled pair of qudits*, which we call an *e-dit*.

$$(1.1a) \quad n \text{ e-dits} + 2n \text{ cdits} \triangleright 2n \text{ qudits}$$

$$(1.1b) \quad n \text{ e-dits} + n \text{ qudits} \triangleright 2n \text{ cdits}$$

The content of the teleportation and superdense coding protocols is captured by (1.1a)-(1.1b) respectively (cf. Bennett’s laws). A *cdit* (also called a *dit*) is the d -ary generalisation of a classical bit, and $X + Y \triangleright Z$ may be read as "resources X and Y can be used to send resource Z ". We briefly summarise the protocols for $n = 1$. In the following, let A and B denote fixed, disjoint regions of a quantum system; they respectively contain qudits q_1, q_2 which are maximally entangled.

- (a) *Teleportation.* A third qudit q_0 with density operator ρ_0 is contained in A , and can be sent to B as follows: q_0, q_1 are measured in an entangled basis, yielding cdits i, j which are sent to B . A unitary U_{ij} (conditioned on i, j) is locally applied to q_2 , whence q_2 has state ρ_0 .
- (b) *Superdense coding.* A unitary U_{ij} (conditioned on chosen cdits i, j) is locally applied to q_1 . Then, q_1 is sent to B , and q_1, q_2 are measured in an entangled basis, yielding cdits i, j .

A and B are typically represented by people named *Alice* and *Bob*, who possess (rather than engulf) qudits. One might also designate a middle-man *Charlie*, who distributes the maximally entangled qudits beforehand.⁶ We adopt this presentation in the sequel. The case with the most obvious practical applications is $d = 2$ (where we have bits, qubits, ebits): each qubit is encoded by a pair of Ising anyons.

1.2.1. With braiding. Let us first mention the work that has already been done in this direction. Huang et al. (2021) performed a quantum simulation (using superconducting qubits) of teleportation in a system of MZMs whose gates are realised by braiding of modes. In the simulated system, each qubit is encoded in a pair of MZMs at the ends of a Kitaev chain [8].

Teleporting the state of N Ising anyons using braiding was studied by Xu & Zhou (2022) [9]. The authors present their results in the context of 2 Ising theories coming from Ising fusion rules (3.1), where Ising anyon q has topological spins $\vartheta_q = e^{i\pi/8}, e^{9i\pi/8}$. We prove a slight variation of their result by implementing the protocol using a different architecture: no braiding is required until Bob’s correction step. Our exposition is presented in the context of all 8 theories coming from the Ising fusion rules (which, by a slight abuse of terminology, we henceforth refer to as ‘Ising theories’). We also formulate the superdense coding protocol in the context of Ising theories with braiding.

1.2.2. Without braiding. Our main contribution is a *braid-free implementation* of both protocols. This should significantly lessen the constraints on the required degree of control over the anyonic system: in principle, we should only require the ability to

- (1) *Pair-create* anyons from the vacuum
- (2) *Fuse* adjacent anyons
- (3) *Measure* fusion outcomes

Since these operations solely rely on the fusion structure of Ising theories, our implementation should naturally carry over to the setting of MZMs. Moreover, we present these protocols in a d -ary context (where $d = 2^n$ for $n \geq 1$) coming from a family of anyon theories: qudits are encoded in a pair of *Tambara-Yamagami* anyons (defined in Section 5.1), and Ising qubits are recovered as a special case ($n = 1$).

1.2.3. Exploiting fusion structure. Suppose we have at our disposal a system of anyons whose braiding operations are universal for computation (or in the qubit case, satisfy the weaker requirement of generating the Clifford group). Then one might question the value of constructing explicit implementations of these protocols, as the quantum gates for both circuits can be converted to braids via the standard compilation approach (using the Solovay-Kitaev algorithm).

Recall that one of our motivating factors is to construct procedures that are as simple as possible, so as to be amenable to near-term realisation. We posit that a key step towards this is to strip

⁶Of course, there is the possibility that Charlie is one of Alice or Bob.

away the need to realise (potentially intricate)⁷ braids. The simplicity of our construction hinges on the *rich fusion structure* of Tambara-Yamagami categories: pairs of anyons can be maximally entangled, simply through recoupling.

1.2.4. Caveats.

1. *Measurement.* In braid-free implementations of the protocols, we assume that measurement can be performed without braiding.⁸ For example, this might be done by bringing two anyons close together and measuring their energy.
2. *Size of encoding space.* We reiterate that in the d -ary setting, $d \in \{2^n : n \geq 1\}$. This restriction is imposed by the fact that $\text{TY}(G)$ (a Tambara-Yamagami category with respect to group G)⁹ admits a braiding if and only if $G \cong \mathbb{Z}_2^n$ [12, Theorem 1.2 (1)]. In this paper, the implementation of protocols is always discussed in the setting of a theory of anyons corresponding to $\text{TY}(\mathbb{Z}_2^n)$. Ising theories are given by $n = 1$. See also Section 5.1.
3. *Universality.* Perhaps universality for computation is of little relevance given our motivations, but we mention it anyway. It is well-known that Ising theories are not universal; by [13, Corollary 4.3], nor is $\text{TY}(\mathbb{Z}_2^2)$. To the author's knowledge, it is open whether $\text{TY}(\mathbb{Z}_2^n)$ are universal when $n > 2$ (though the Property F conjecture [13] suggests they are not).¹⁰

1.3. Main results and outline of paper. We briefly outline the contents of each of the sections that follow, and state the main theorems therein. An outline of the subsections that comprise Section 3 and Section 5 is found at their respective outset.

In Section 2, we review the algebraic theory of anyons and its accompanying graphical calculus.

In Section 3, we determine a procedure for the teleportation of (multiple) Ising qubits *with braiding*. That is, we prove the following theorem which is a variation of the result of [9].

Theorem 3.1 (Teleportation using Ising anyons and braiding). *The fusion state of $2p$ Ising anyons (that is, a p -qubit state) can be teleported via the procedure shown in Figure 11. In particular, braiding is not required anywhere other than the correction step.*

In Section 4, we determine a procedure for the superdense coding of bits using Ising anyons *and braiding*. That is, we prove the following theorem.

Theorem 4.1 (Superdense coding using Ising anyons and braiding). *We can realise the superdense coding protocol using Ising anyons, as shown in Figure 15. In particular, braiding is not required anywhere other than the 2-bit encoding step.*

In Section 5, we generalise the protocols of Sections 3 and 4 to a d -ary setting for $d \geq 2$ (where $d = 2^n$ as per the caveat in Section 1.2.4) using *Tambara-Yamagami anyons* (of which Ising anyons are a special case), and remove the reliance on braiding. Then, in principle, both protocols should be realisable given capabilities (1)-(3) from Section 1.2.2. The following theorems are proved.

Theorem 5.1 (Braid-free qudit teleportation using Tambara-Yamagami anyons). *Consider a Tambara-Yamagami theory of rank $d + 1$ where $d = 2^n$. The fusion state of N Tambara-Yamagami anyons (that is, an $N/2$ -qudit state, where N is even) can be teleported via the procedure shown in Figure 18. In particular, no braiding is required.*

Theorem 5.2 (Braid-free Pauli gates for Ising qubits). *We can apply Pauli gates to an Ising qubit without braiding. The (braid-free) Pauli gates $\{I, X, Y, Z\}$ are realised by U_{g_1, g_2} as defined in equation (5.1), for $g_1, g_2 \in \mathbb{Z}_2$.*

⁷For instance, see the realisation of the entangling 2-qubit CNOT gate by braiding of Fibonacci anyons (which are universal for computation) [10, Figure 3].

⁸Some schemes for charge measurement involve Mach-Zehnder-like interferometry, wherein a probe anyon effectively winds around the region of interest, e.g. [11].

⁹Where G is finite and abelian by definition.

¹⁰There exists a scheme for supplementing Ising anyons with non-topological operations in order to achieve universality [14, 15]. Similarly, a hybrid approach has also been discussed for MZMs [16, 17].

Theorem 5.3 (Braid-free d -ary superdense coding using Tambara-Yamagami anyons). Consider a Tambara-Yamagami theory of rank $d + 1$ where $d = 2^n$. We can realise the d -ary superdense coding protocol using Tambara-Yamagami anyons, as shown in Figure 22(i). In particular, braiding is not required anywhere other than the 2-dit encoding step.

1.4. Teleportation and information flow. In this section, we roughly sketch some ideas that become clearer in the main exposition. Consider the two spacetime processes for a system of anyons in Figure 1. Time runs downwards in all of our diagrams, and the label accompanying the worldline of an anyon denotes its charge. We have the freedom to simultaneously reverse the orientation assigned to an edge (that is, a segment of worldline which is unidirectional with respect to the time-axis) and invert the charge of its accompanying label.

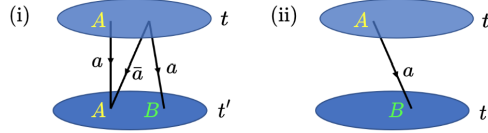


FIGURE 1. Anyonic systems with highlighted timeslices t, t' where $t' > t$. Spatial points A, B denote fixed locations in the system. (i) An antiparticle-particle pair are initialised from the vacuum at time t . A particle of charge a lying at point A annihilates with its anti-particle \bar{a} at time t' . (ii) Particle a is dragged from A to B .

The two diagrams differ by a phase t_a called the *pivotal coefficient* of a (see Section 2.7). That is, the process in (i) is physically equivalent to the one shown in (ii). This equivalence leads one to question whether the particle in (i) is, in some sense, ‘teleported’ from A to B upon annihilation with its antiparticle.¹¹ Suppose the state of the particle at A immediately before its annihilation is $|\psi\rangle$. As a necessary condition for ‘teleportation’, we would expect that the particle at B assumes state $|\psi\rangle$ immediately after time t' (i.e. that $|\psi\rangle$ is *quantum-teleported* from A to B at time t').^{12,13} This condition provides no physical insight in the case of one anyon, which always has a 1-dimensional state space. The narrative becomes more compelling in the case of two (or more) anyons, where we assume both anyons to be nonabelian (so that their state space has dimension $d > 1$).

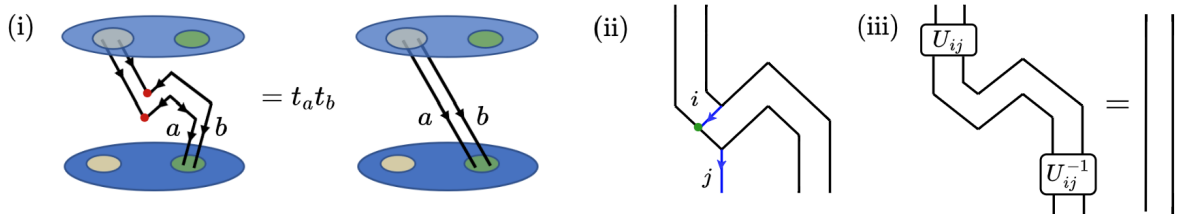


FIGURE 2. The diagrams in (i) differ by a phase $t_a t_b$, whence the process on the left-hand side teleports the state of *nonabelian* anyons a and b from the yellow to the green region of the system. In (ii)-(iii), black worldlines represent self-dual nonabelian anyons of charge q , and blue edges represent a fusion outcome of a pair of q anyons. In (iii), the coupon U_{ij} denotes an invertible \mathbb{C} -linear operator whose indices i, j are each indexed by the possible fusion outcomes of a pair of q anyons.

¹¹Here, we place quotation marks around ‘teleport’ (which has no clear definition) in order to distinguish it from (*quantum*) *teleportation* of states (which is well-defined).

¹²One might argue that this is also a sufficient condition for ‘teleportation’. That is, if the state of the particle is teleported, then we say that the particle itself is ‘teleported’ since its state encodes all of its measurable properties.

¹³We warn the reader that this comment is philosophical in nature. In one school of thought, ‘teleportation’ of an object from a point A to a point B in a connected space \mathcal{M} , requires that the object appearing at B is the ‘same’ as the one from point A . It is further stipulated that an object retains its ‘sameness’ over a time interval $[t, t']$ given that its worldline defines a continuous function $f : [t, t'] \rightarrow \mathcal{M}$. While the worldline in Figure 1(ii) is in accord with this stipulation, the worldline in (i) is not. Suppose we modify the stipulation as follows: an object retains its ‘sameness’ over time interval $[t, t']$ if its worldline is given by a continuous function $\gamma : \mathbb{R} \rightarrow \mathcal{M} \times [t, t']$. In this case, (i) and (ii) both satisfy ‘sameness’. A physical theory which cannot distinguish between the state of a particle (or collection of particles) undergoing processes (i)-(ii), might thus be regarded as favouring the second notion of ‘sameness’. Indeed, anyon theories are one such example.

Indeed, we see that the state of the pair of particles in Figure 2(i) is teleported by a process of the same form as in Figure 1(i), as the process coincides with the identity operator (up to a global phase). However, note that there may be an *obstruction* to teleportation if the fusion outcomes at the red-coloured vertices in Figure 2(i) are nontrivial, which occurs with nonzero probability. We apply the following three constraints to a and b .

- (1) All possible fusion outcomes of a and b are abelian.
- (2) All possible fusion outcomes of a and b occur without multiplicity.
- (3) Let $a = b = q$, where $q = \bar{q}$ (i.e. q is its own antiparticle).

Then, the process on the left-hand side of the equality in diagram (i) can be redrawn as (ii); each of the labels i, j are indexed by the possible fusion outcomes of a pair of q anyons. Assumption (1) guarantees the absorption of any fusion outcome i at the green-coloured vertex.

Suppose the pair of q anyons are initially in state $|\psi\rangle$ in diagram (ii). It turns out that the occurrence of obstructions i, j is physically equivalent to the teleportation of $|\psi\rangle$ up to an invertible operator U_{ij} , where $U_{00} = \text{id}$; then $|\psi\rangle$ can be recovered by applying U_{ij}^{-1} (see Figure 2(iii)). This line of thought is made precise in Sections 5.2.2-5.2.3.

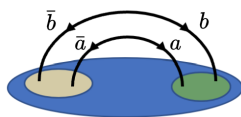


FIGURE 3

Remark 1.1.

- (i) Under assumptions (1)-(2), we are guaranteed maximal entanglement between the two pairs of anyons in the yellow and green regions of the system in Figure 3; see Section 3.2.1.
- (ii) Suppose that in addition to assumptions (1)-(3), we further assume that all possible fusion outcomes are self-dual. Then q is a *Tambara-Yamagami anyon* (see Section 5.1), and the coupons U_{ij} in Figure 2(iii) are always unitary (Corollary 5.12).

Remark 1.2 (Information flow and pivotal structure). Teleportation manifests as a zigzag-like flow of quantum information in spacetime. We note that Figure 2(iii) is reminiscent of Abramsky & Coecke’s formulation of quantum teleportation in the setting of rigid monoidal categories (2004) [18]; see also [19, 20]. The information flow in the anyonic setting is tied to the *pivotal structure* of the underlying fusion category.

1.5. Acknowledgements. The author would like to thank Dmitri Nikshych and David Penneys for pointing him towards results on Tambara-Yamagami categories that are key to the exposition of this paper. The author is grateful for the support of Tamkeen under the NYU Abu Dhabi Research Institute grant CG008. This work is dedicated to M. Hilby.

2. REVIEW OF ALGEBRAIC THEORY OF ANYONS

At least to the extent relevant for the sections that follow, we review the algebraic theory of anyons and its accompanying graphical calculus. A comprehensive introduction is found in [21, 22].

A theory of anyons has an underlying finite set of labels $\mathfrak{L} = \{0, a, b, \dots\}$ that represent their distinct possible ‘types’ or (*topological*) *charges*. Trivial label 0 represents the vacuum. Anyons can

- (1) *Braid*, i.e. a sequence of particle exchanges represented as worldlines in (2+1)-dimensions.
- (2) *Twist*, i.e. a 2π self-rotation of specified orientation.
- (3) *Fuse*. Two anyons of charge a and b can generally have total charge $a \times b = \sum_c N_c^{ab} c$ where fusion coefficients $N_c^{ab} \in \mathbb{Z}_{\geq 0}$ are *finite*. Fusion ‘ \times ’ is *commutative* and *associative*. The summation indicates that the total charge of two or more anyons is possibly a *superposition* of charges. It always holds that $\sum_c N_c^{ab} \geq 1$ and $N_b^{a0} = N_b^{0a} = \delta_{ab}$. Each $a \in \mathfrak{L}$ has a unique *dual* charge \bar{a} such that $N_0^{a\bar{a}} = N_0^{\bar{a}a} = 1$. Coefficients N_c^{ab} satisfy symmetries (2.1).¹⁴

$$(2.1) \quad \text{(i) } N_c^{ab} = N_c^{ba} \quad , \quad \text{(ii) } N_c^{ab} = N_a^{b\bar{c}} = N_b^{\bar{c}a} \quad , \quad \text{(iii) } N_c^{ab} = N_c^{\bar{b}\bar{a}}$$

¹⁴Symmetries (i) and (ii) respectively come from the commutativity and associativity of fusion; (iii) is CPT symmetry and is seen through application of leg-bending operators (Section 2.6).

2.1. Fusion spaces and quantum dimension. The fusion Hilbert space of a and b is given by $V^{ab} \cong \bigoplus_c V_c^{ab}$ where $\dim(V_c^{ab}) = N_c^{ab}$. Measuring the charge of such a pair projects their state to a subspace V_c^{ab} . The dual space of V_c^{ab} is denoted V_{ab}^c ; its orthogonal basis elements can be thought of as the distinguishable ways in which a pair a and b may be initialised from c . Spaces of the form V_c^{ab}, V_{ab}^c are called *triangular*. Trivalent vertices represent their orthonormal basis elements.¹⁵

$$(2.2) \quad V_c^{ab} = \text{span} \left[\begin{array}{c} a \quad b \\ \diagdown \quad / \\ \mu \\ | \\ c \end{array} \right]_{\mu=1}^{N_c^{ab}}, \quad V_{ab}^c = \text{span} \left[\begin{array}{c} c \\ / \quad \backslash \\ a \quad b \end{array} \right]_{\mu=1}^{N_c^{ab}}$$

Our convention is that diagrams should be parsed from *top-to-bottom* (i.e. the time axis runs *downwards*). Any given line will be accompanied by a label $a \in \mathfrak{L}$ (unless it is obvious what the label should be) and should be interpreted as the worldline of an anyon with charge a ; when $a = 0$, the worldline is either dashed or omitted altogether. We may sometimes direct worldlines for clarity; directing a worldline with a self-dual label is superfluous. In (2.3), we give diagrammatic expressions in V^{ab} for (i) orthogonality, and (ii) the completeness relation (i.e. identity operator); given a, b fixed, note that the set of all elements of form (iii) defines an orthonormal basis of $\text{End}(V^{ab})$ with respect to the trace inner product.

$$(2.3) \quad \begin{array}{ccc} \text{(i)} & \text{(ii)} & \text{(iii)} \\ \begin{array}{c} c \\ | \\ \mu \\ \circ \\ | \\ \mu' \\ c' \end{array} = \delta_{c,c'} \delta_{\mu,\mu'} & \begin{array}{c} a \quad b \\ | \quad | \\ = \sum_{c,\mu} \begin{array}{c} a \quad b \\ \diagdown \quad / \\ \mu \\ | \\ c \\ / \quad \backslash \\ a \quad b \end{array} \end{array} & \begin{array}{c} a \quad b \\ \diagdown \quad / \\ \mu \\ | \\ c \\ / \quad \backslash \\ a \quad b \end{array} \end{array}$$

The amplitude of an unnormalised loop labelled by a is the *quantum dimension* $d_a > 0$ of a . The quantum dimensions of a theory will satisfy (2.4a)-(2.4b).¹⁶

$$(2.4a) \quad d_a = \begin{array}{c} \circlearrowright \\ a \end{array} = \begin{array}{c} \circlearrowleft \\ \bar{a} \end{array} = d_a \quad (2.4b) \quad d_a d_b = \sum_c N_c^{ab} d_c$$

Note that $d_0 = 1$. A charge a is called *abelian* if $\sum_c N_c^{ab} = 1$ for all $b \in \mathfrak{L}$ (equivalently, $a \times a = 0$); else it is called *nonabelian*. We see that $d_a = 1$ for a abelian; else, $d_a \geq \sqrt{2}$. Unless stated otherwise, all trivalent vertices (2.2) implicitly carry a normalisation factor $(d_c/d_a d_b)^{1/4}$ in our diagrams.

We write the fusion space of $k \geq 2$ anyons a_1, \dots, a_k as in (2.5); the possible values for their total charge is independent of the order in which they are fused (by associativity), and are indexed here by c . Such a space can be understood by decomposing it into triangular spaces as in (2.6).

$$(2.5) \quad V^{a_1, \dots, a_k} \cong \bigoplus_c V_c^{a_1, \dots, a_k}$$

A collection of k anyons can be pairwise fused in C_{k-1} different ways, where C_k is the k^{th} Catalan number.¹⁷ Each distinct sequence defines a *fusion basis*.¹⁸ Such a basis specifies a decomposition of the k -anyon space, and amounts to a choice of measurement basis. By associativity of fusion, all such decompositions are isomorphic, e.g. there are two fusion bases when $k = 3$.

$$(2.6) \quad V_d^{abc} \cong \bigoplus_e V_e^{ab} \otimes V_d^{ec} \cong \bigoplus_f V_d^{af} \otimes V_f^{bc}$$

¹⁵The multiplicity index (typically Greek, given here by μ) next to the vertex is omitted when $N_c^{ab} = 1$.

¹⁶From (2.4b) and the Frobenius-Perron theorem for nonnegative matrices, one can deduce that d_a is the largest positive eigenvalue of matrix N^a where $[N^a]_{bc} := N_c^{ab}$.

¹⁷ C_{k-1} can also be thought of as counting distinct parenthesisations of a length k string.

¹⁸Graphically, a k -particle fusion basis is a full binary tree with k leaves. There are two trees for $k = 3$ – see (2.7).

2.2. F and R-matrices.¹⁹ A change of fusion basis is realised by (some sequence of) so-called *F-matrices*, which are unitary since they transform between orthonormal bases. An *F-matrix recouples* a triple of objects, i.e. $F_d^{abc} : \bigoplus_e V_e^{ab} \otimes V_d^{ec} \xrightarrow{\sim} \bigoplus_f V_d^{af} \otimes V_f^{bc}$ is given by (2.7), and its inverse is written G_d^{abc} . Then we can deduce that $(F_d^{abc})^* : \bigoplus_e V_{ab}^e \otimes V_{ec}^d \xrightarrow{\sim} \bigoplus_f V_{af}^d \otimes V_{bc}^f$.

$$(2.7) \quad \begin{array}{c} a & b & c \\ & \mu_1 & \\ & e & \\ & \mu_2 & \\ & & d \end{array} = \sum_{f, \nu_1, \nu_2} [F_d^{abc}]_{(f, \nu_1, \nu_2), (e, \mu_1, \mu_2)} \begin{array}{c} a & b & c \\ & & \nu_1 \\ & f & \\ & & \nu_2 \\ & & d \end{array}, \quad G_d^{abc} := (F_d^{abc})^{-1}$$

A clockwise exchange of two anyons a and b is described by the *R-matrix* $R_c^{ab} : V_c^{ab} \xrightarrow{\sim} V_c^{ba}$ where $R_c^{ab} = \bigoplus_c R_c^{ab}$. Diagrammatically, $R_c^{ab} : V_c^{ab} \xrightarrow{\sim} V_c^{ba}$ is given by (2.8)(i). Then R_c^{ab} is given by (2.8)(ii), which can be seen by stacking the crossing on top of the identity operator for V_c^{ba} .

$$(2.8) \quad (i) \quad R_c^{ab} : \begin{array}{c} a & b \\ & \mu \\ & c \end{array} \mapsto \begin{array}{c} a & b \\ & \mu \\ \mu & \\ & c \end{array} = \sum_{\nu} [R_c^{ab}]_{\nu\mu} \begin{array}{c} a & b \\ & \nu \\ & c \end{array} \quad (ii) \quad R_c^{ab} : \begin{array}{c} a & b \\ | & | \\ | & | \end{array} \mapsto \begin{array}{c} a & b \\ \diagdown & \diagup \\ & \nu \\ \diagup & \diagdown \\ c & \mu \\ & a \end{array} = \sum_{c, \mu, \nu} [R_c^{ab}]_{\nu\mu} \begin{array}{c} a & b \\ & \nu \\ c & \mu \\ & a \end{array}$$

An anticlockwise exchange of a and b is given by $(R^{-1})^{ab} := (R^{ba})^{-1}$. Since *R-matrices* describe evolutions of quantum states, we require that they are unitary: given the unitarity of *F-matrices*, this turns out to be automatically satisfied [30].^{20,21} We always have that $R^{a0} = R^{0a} = 1$.

2.3. Pentagon and hexagon equations. In order for the *F* and *R-matrices* to be consistently defined, they must satisfy compatibility conditions known as the *pentagon* and *hexagon* axioms. There are two distinct hexagon axioms, which we respectively denote by H1 and H2 in Figure 4.

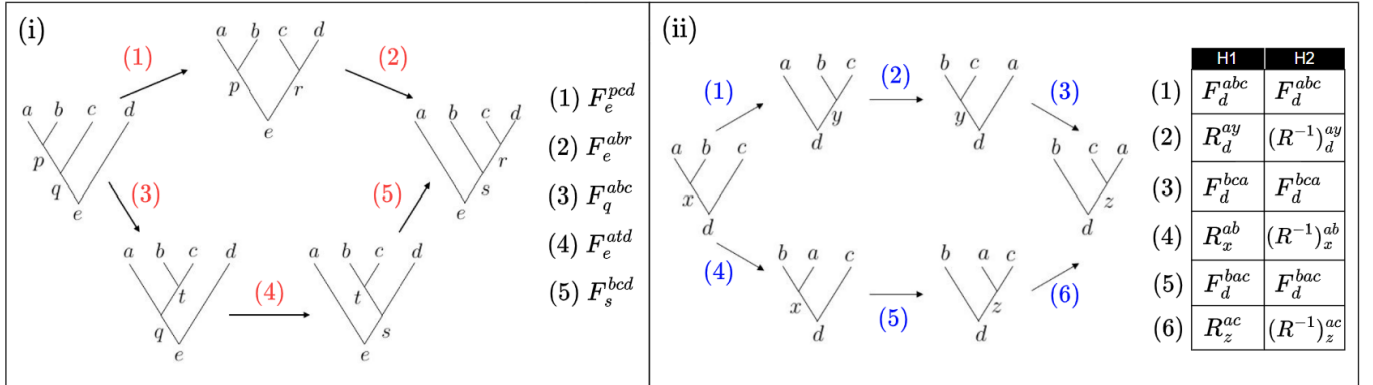


FIGURE 4. Arrows map between fusion spaces, all of which have a specified decomposition. The pentagon and hexagon axioms respectively demand that the diagrams in (i) and (ii) commute for all possible labellings.

By fixing a choice of fusion states in the initial and final spaces (given a permissible choice of labels) in (i)-(ii) above, we obtain an entry-wise form of the compatibility conditions. This results in a system of equations called the pentagon and hexagon equations. For instance, if the triangular spaces in (i)-(ii) are all 1-dimensional for the given choices of labels, these equations take form (2.9)-(2.10).²² In the presence of triangular spaces with dimension greater than 1, they become considerably more unwieldy, e.g. see [23, Appendix D].

$$(2.9) \quad [F_e^{abr}]_{sp} [F_e^{pcd}]_{rq} = \sum_t [F_s^{bcd}]_{rt} [F_e^{atd}]_{sq} [F_q^{abc}]_{tp}$$

¹⁹The entries of *F* and *R-matrices* are respectively called *F* and *R-symbols*.

²⁰Here, the unitarity postulate of quantum mechanics is obviated by the postulate that state spaces are Hilbert.

²¹As a linear operator, R^{ab} is technically a linear isometry since it maps between two distinct spaces for $a \neq b$. Its matrix representation is unitary.

²²For a *multiplicity-free* theory (i.e. all fusion coefficients take value in $\{0, 1\}$), its consistency equations are given by (2.9)-(2.10) for all possible label choices.

$$(2.10a) \quad \sum_y [F_d^{bca}]_{zy} [R_d^{ay}] [F_d^{abc}]_{yx} = [R_z^{ac}] [F_d^{bac}]_{zx} [R_x^{ab}]$$

$$(2.10b) \quad \sum_y [F_d^{bca}]_{zy} [(R^{-1})_d^{ay}] [F_d^{abc}]_{yx} = [(R^{-1})_z^{ac}] [F_d^{bac}]_{zx} [(R^{-1})_x^{ab}]$$

Remark 2.1.

- (i) It follows from the hexagon axioms that (a) string diagrams in the graphical calculus enjoy equivalence under the 2^{nd} and 3^{rd} Reidemeister moves, and (b) strands may slide over (or under) trivalent vertices.
- (ii) Technically, there is another compatibility condition called the *triangle axiom* which ensures that fusion with the vacuum is trivial.²³ This axiom is equivalent to levying the ('obvious') condition that all F -matrices F_d^{abc} where any of a, b, c coincide with 0, are the identity.

2.4. Topological spin. Performing a clockwise 2π -twist of an anyon a accumulates a phase factor $\vartheta_a \in U(1)$; a quantity known as the *topological spin* of a . We always have $\vartheta_0 = 1$.

$$(i) \quad \begin{array}{c} \text{clockwise} \\ \text{kink} \end{array} = \begin{array}{c} \text{anticlockwise} \\ \text{kink} \end{array} = \vartheta_a \Big|_a \quad (ii) \quad \begin{array}{c} \text{anticlockwise} \\ \text{kink} \end{array} = \begin{array}{c} \text{clockwise} \\ \text{kink} \end{array} = \vartheta_a^* \Big|_a$$

FIGURE 5. *Kinks* represent (i) clockwise and (ii) anticlockwise 2π -twists of a .

The endomorphism $M^{ab} := R^{ba} \circ R^{ab}$ describes the (clockwise) *monodromy* of a and b , and M_c^{ab} is its restriction to V_c^{ab} . Topological spins always satisfy (2.11a)-(2.11b). A result of Vafa tells us that any topological spin is a root of unity [24].²⁴ It follows that for any a, b , we have that $(M^{ab})^n = \text{id}$ for some $n \geq 1$.

$$(2.11a) \quad [M_c^{ab}]_{\mu\nu} = \sum_\lambda [R_c^{ba}]_{\mu\lambda} [R_c^{ab}]_{\lambda\nu} = \frac{\vartheta_c}{\vartheta_a \vartheta_b} \delta_{\mu\nu} \quad (2.11b) \quad \vartheta_a = \vartheta_{\bar{a}}$$

$$(i) \quad R^{ba} \circ R^{ab} = \begin{array}{c} \text{Y-junction} \\ \text{with twist} \end{array} = \begin{array}{c} \text{Y-junction} \\ \text{with twist} \end{array} = \begin{array}{c} \text{Y-junction} \\ \text{with twist} \end{array} = \frac{\vartheta_c}{\vartheta_a \vartheta_b} \begin{array}{c} \text{Y-junction} \\ \text{without twist} \end{array} \quad (ii) \quad \begin{array}{c} \text{twisted loop} \\ \text{with twist} \end{array} = \begin{array}{c} \text{twisted loop} \\ \text{without twist} \end{array}$$

FIGURE 6. Promoting worldlines to worldribbons, kinks in Figure 5 can be tautened to 2π -twists. We respectively illustrate identities (2.11a)-(2.11b) using worldribbons. (i) The middle equality is seen by pulling taut the ribbon from the tops and bottom. (ii) We must be able to push twists around a closed loop. If we do the same but with kinks and worldlines, we recover the equivalence of kinks as in Figure 5.

2.5. S-matrix. The *S-matrix* of a theory of anyons is given by (2.12), where $\mathcal{D} = \sqrt{\sum_c d_c^2}$ is the *total quantum dimension* of the theory.

$$(2.12) \quad [S]_{ab} := \frac{1}{\mathcal{D}} \left(\text{braiding of } a \text{ and } b \right) = \frac{1}{\mathcal{D}} \sum_c \frac{\vartheta_c}{\vartheta_a \vartheta_b} N_c^{a\bar{b}} d_c, \quad a, b \in \mathfrak{L}$$

Remark 2.2 (Braiding nondegeneracy and modularity).

- (i) A charge x is called *transparent* if its monodromy with any charge a is trivial, and a theory of anyons said to have a *nondegenerate braiding* if the only transparent charge is 0.
- (ii) Let \mathbf{s}_x denote a column vector of S , i.e. $[\mathbf{s}_x]_a = [S]_{ax}$. A charge x is transparent if and only if $\mathbf{s}_x = d_x \mathbf{s}_0$ [22, Lemma E.13]. It follows that $\text{nul}(S) \geq t$, where t is the number of nontrivial transparent charges. It is actually sufficient to have $t = 0$ in order for S to invertible .

²³A further discussion of the triangle axiom (or 'fundamental triangle equation') is found in [22, Section E.1.2].

²⁴A proof of Vafa's result may also be found in [22, Theorem E.10].

(iii) A theory is called *modular* if its S -matrix is unitary. A theory is modular if and only if it has nondegenerate braiding (i.e. $t = 0$) [22, Section E.5].

2.6. Leg-bending operators. For all a, b, c , there exist linear maps $K_c^{ab}, L_c^{ab}, K_{ab}^c, L_{ab}^c$ as defined in (2.13). We call them the *leg-bending operators*.

$$(2.13a) \quad K_c^{ab} : V_c^{ab} \longrightarrow V_{\bar{a}\bar{c}}^b \quad L_c^{ab} : V_c^{ab} \longrightarrow V_{\bar{c}\bar{b}}^a$$

$$(2.13b) \quad K_{ab}^c : V_{ab}^c \longrightarrow V_{\bar{a}\bar{b}}^{\bar{c}} \quad L_{ab}^c : V_{ab}^c \longrightarrow V_{\bar{a}\bar{b}}^{\bar{c}}$$

The leg-bending operators are isometries (unitary matrices) and satisfy (2.14a) [22, Theorem E.6]. This commutative diagram can be seen as a compatibility condition for CPT transformations.²⁵ Equation (2.14b) is called the *pivotal identity*, where equalities (i) and (ii) can respectively be seen by completing an anticlockwise and clockwise loop of (2.14a).²⁶

$$(2.14a) \quad \begin{array}{ccc} & V_c^{ab} & \\ K_c^{ab} \swarrow & & \searrow L_c^{ab} \\ V_{\bar{a}\bar{c}}^b & & V_{\bar{c}\bar{b}}^a \\ L_{\bar{a}}^{b\bar{c}} \uparrow & & \uparrow K_{\bar{b}}^{\bar{c}a} \\ V_{\bar{a}}^{b\bar{c}} & & V_{\bar{b}}^{\bar{c}a} \\ K_{\bar{a}}^{b\bar{c}} \downarrow & & \downarrow L_{\bar{b}}^{\bar{c}a} \\ & V_{\bar{a}\bar{b}}^{\bar{c}} & \end{array}$$

$$(2.14b) \quad \text{Diagrammatic identity showing two ways to complete a loop of vertices, resulting in the same strand configuration.$$

The entries of leg-bending matrices are given by F -symbols (2.15)-(2.16).²⁷

$$(2.15a) \quad [K_c^{ab}]_{\nu\mu} = \sqrt{\frac{d_a d_b}{d_c}} [F_b^{\bar{a}ab}]_{(c,\mu,\nu),0}^* \quad (2.15b) \quad [L_c^{ab}]_{\nu\mu} = \sqrt{\frac{d_a d_b}{d_c}} [F_a^{abb}]_{0,(c,\mu,\nu)}$$

$$(2.16a) \quad K_{ab}^c = (K_c^{ab})^* \quad (2.16b) \quad L_{ab}^c = (L_c^{ab})^*$$

Remark 2.3.

- (i) Identity (2.4b) for quantum dimensions follows from the unitarity of the matrices in (2.15).
- (ii) The composition of oppositely oriented kinks can be transformed to the identity strand using the 2nd and 3rd Reidemeister moves, along with the pivotal identity (2.14b).

2.7. Pivotal coefficients. The quantity $t_a \in \mathbb{C}$ from (2.17) is called the *pivotal coefficient* of a .

$$(2.17) \quad \text{Diagrammatic equation for pivotal coefficient } t_a \text{ involving } F_a^{a\bar{a}a} \text{ and } d_a.$$

Then noting that $L_{\bar{0}}^{a\bar{a}} = d_a [F_a^{a\bar{a}a}]_{\bar{0}\bar{0}}^* = t_a$, we see that

$$(2.18) \quad \text{Diagrammatic equation showing the pivotal coefficient } t_a \text{ and its adjoint } t_a^* \text{ on strands.$$

²⁵Here, CPT symmetry is the preservation of inner products under an inversion of charge, parity and time. CPT transformations can be realised via two orientations, which are not isotopic in $(2+1)\text{D}$; equality is given by (2.14a). CPT transformations can be performed on any Hom-space via leg-bending, with consistency ensured by (2.14a).

²⁶This identity can also be seen to follow from the triviality of 2π -twisting three anyons with total charge 0 [21].

²⁷Derivations in the multiplicity-free case are found in [25, Section 6.2]; they follow analogously with multiplicity.

For any a , the pivotal coefficients satisfy (2.19). Equation (2.19a) follows from the unitarity of the leg-bending operators, and (2.19b) from commutative diagram (2.14a) with a or b set to 0.

$$(2.19a) \quad |t_a| = 1 \qquad (2.19b) \quad t_{\bar{a}} = t_a^*$$

When a is self-dual, its pivotal coefficient is called the *Frobenius-Schur indicator* of a and is written as \varkappa_a . Note that $\varkappa_a = \pm 1$ and $\varkappa_0 = 1$.

Remark 2.4. Zigzags of the form in (2.17) and (2.18) are straight lines (up to a scalar). For this reason, one does not assign the usual normalisation factor of $d_a^{-1/2}$ to their trivalent vertices.

Remark 2.5 (Topological spins revisited). Identities (2.20) relate R -symbols and topological spins via pivotal coefficients, whence it is clear that the F and R -symbols of a theory encode its topological spins. Equation (2.20a) can be seen by replacing the crossing in a clockwise kink with its expansion (2.8)(ii) in the standard basis; then, the result is obtained by applying leg-bending matrices and orthogonality relation (2.3)(i) as appropriate.

$$(2.20a) \quad \vartheta_a = \frac{1}{d_a} \sum_c d_c \operatorname{tr}(R_c^{aa}) \qquad (2.20b) \quad \vartheta_a = t_a(R_0^{\bar{a}a})^*$$

Equation (2.20b) follows from

Theorem 2.6 (Fuchs, Runkel, Schweigert '02). [26] *Take a set S of labels a_1, \dots, a_k such that charge-conjugation is a permutation on S and $k \geq 2$.²⁸ Let $V = V_0^{a_1 \dots a_k}$ and $\omega = \prod_{i=1}^k \omega_i$, where $\omega_i = \varkappa_{a_i}$ if a_i is self-dual, or else $\omega_i = 1$. If $\dim(V)$ is odd, then $\omega = 1$.*

Corollary 2.7.

- (i) For a, b, c self-dual such that N_c^{ab} is odd, we have that $\varkappa_a \varkappa_b \varkappa_c = 1$.
- (ii) For a, c such that c is self-dual and $N_c^{a\bar{a}}$ is odd, we have that $\varkappa_c = 1$.

Proof. Consider Theorem 2.6 for $k = 3$. There are two possible cases: (i) all elements of S are self dual, and (ii) only 1 element of S is self dual. Let $S = \{a, b, c\}$. For (i), we have that $V \cong V_c^{ab}$ with a, b, c self-dual. For (ii), we choose (without loss of generality) c to be self-dual, whence $V \cong V_c^{a\bar{a}}$. The result follows, since we must have $\omega = 1$ in both cases. \square

For example, all theories of anyons considered in the sections that follow have Tambara-Yamagami fusion rules (5.2) for a group $G \cong \mathbb{Z}_2^n$. It is clear that from Corollary 2.7(i) that $\varkappa_g = 1$ for all $g \in G$. Theorem 2.6 follows from the final theorem in [26]. An extended discussion of the role of Frobenius-Schur indicators and their interplay with the graphical calculus can be found in [27].

2.8. Gauge transformations. Explicit F and R -matrices are obtained by fixing an orthonormal basis on triangular spaces, which gives rise to redundancy in our algebraic description. That is, for any space V_c^{ab} , there is a $U(N_c^{ab})$ -freedom in the choice of basis. A change of (orthonormal) basis is called a *gauge transformation*. Let u_c^{ab} denote a gauge transformation on V_c^{ab} , where

$$(2.21) \quad u_c^{ab} : \begin{array}{c} a \quad b \\ \diagdown \quad / \\ \mu \\ | \\ c \end{array} \mapsto \sum_{\mu'} [u_c^{ab}]_{\mu'\mu} \begin{array}{c} a \quad b \\ \diagdown \quad / \\ \mu' \\ | \\ c \end{array}$$

Gauge transformations of F -symbols and R -matrices are given by

$$\begin{aligned} [(F_d^{abc})']_{(f,\nu'_1,\nu'_2),(e,\mu'_1,\mu'_2)} &= \sum_{\mu_1,\mu_2,\nu_1,\nu_2} [u_d^{af}]_{\nu'_2\nu_2} [u_f^{bc}]_{\nu'_1\nu_1} [F_d^{abc}]_{(f,\nu_1,\nu_2),(e,\mu_1,\mu_2)} [(u_e^{ab})^\dagger]_{\mu_1\mu'_1} [(u_d^{ec})^\dagger]_{\mu_2\mu'_2} \\ (R_c^{ab})' &= u_c^{ba} R_c^{ab} (u_c^{ab})^\dagger \end{aligned}$$

which in the absence of multiplicity, become

²⁸That is, the function $\mathcal{C} : S \rightarrow S$ is a bijection, where $\mathcal{C}(a_i) = \bar{a}_i$.

$$(2.22a) \quad [(F_d^{abc})']_{fe} = \frac{u_d^{af} u_f^{bc}}{u_e^{ab} u_d^{ec}} [F_d^{abc}]_{fe} \quad (2.22b) \quad (R_c^{ab})' = \frac{u_c^{ba}}{u_c^{ab}} R_c^{ab}$$

Transformations satisfy (2.23) in accord with the triviality of fusion and braiding with the vacuum.

$$(2.23) \quad u_a^{a0} = u_a^{0a} = 1$$

Remark 2.8 (Gauge-invariance). We generally do not expect gauge-variant quantities to correspond to physical observations, which lends importance to *gauge-invariants*, e.g. (i) monodromies; (ii) R -symbols R_b^{aa} for $N_b^{aa} = 1$; (iii) topological spins; (iv) F -symbols $[F_b^{abc}]_{bb}$. From (iv), we deduce that Frobenius-Schur indicators are gauge-invariant.

2.9. Anyon theories. Let (\mathcal{L}, \times) denote a set of labels with fusion coefficients as defined above. A *theory of anyons* is defined by a corresponding set of unitary F and R -matrices up to gauge equivalence; that is, a gauge class of unitary solutions to the pentagon and hexagon equations. If (\mathcal{L}, \times) admits at least one theory of anyons, it is called an *anyon model*, and the *rank* of such a theory is $|\mathcal{L}|$. A theory of anyons is precisely a unitary ribbon fusion category \mathcal{C} , and the underlying set of F and R -symbols is called the *skeletal data* of \mathcal{C} .

3. TELEPORTATION OF QUBITS BY BRAIDING ISING ANYONS

In this section, we consider the realisation of the teleportation protocol via braiding Ising anyons. This was recently studied by Xu & Zhou in [9]; we present a variation on the architecture used there. In particular, braiding will not be required until the recipient (Bob) applies corrections to his qubits. The primary goal of this section is to prove the following theorem.

Theorem 3.1. *The fusion state of $2p$ Ising anyons (that is, a p -qubit state) can be teleported via the procedure shown in Figure 11. In particular, braiding is not required anywhere other than the correction step.*

We first analyse the single-qubit case (Section 3.2), and then proceed to multi-qubit teleportation (Section 3.3). As part of our exposition, we introduce a toy model (*'noughts and crosses'*) as an aid for understanding the correction of Pauli-X errors (Section 3.3.1). Let us begin by introducing the Ising theories.

3.1. Ising theories. Suppose we wish to realise a qubit whose logical basis corresponds to the fusion outcomes (say, the vacuum '0' and an abelian anyon '1') of a pair of anyons with like-charge ' q '. I.e. the underlying fusion rule is (3.1a), whence fusion rules (3.1b) can be deduced via symmetries (2.1).

$$(3.1a) \quad q \times q = 0 + 1$$

$$(3.1b) \quad 1 \times 1 = 0 \quad , \quad q \times 1 = 1 \times q = q$$

There are 8 theories of anyons realised by the above fusion rules, all of which are modular. Half of these are called *Ising* theories and have $\varkappa_q = 1$, while the other half have $\varkappa_q = -1$ and are called $SU(2)_2$ theories. We see from (2.4b) that $d_q = \sqrt{2}$. By an abuse of terminology, we will refer to all 8 theories as Ising, and will call q an Ising anyon in each of these.

We use the standard column vector representation $(\alpha, \beta)^T$ for an Ising qubit $|\varphi\rangle = \alpha|0\rangle + \beta|1\rangle$. Fixing a choice of gauge, the nontrivial F -symbols of any Ising theory are

$$(3.2) \quad F_q^{qqq} = \frac{\varkappa_q}{\sqrt{2}} \begin{pmatrix} 1 & 1 \\ 1 & -1 \end{pmatrix} \quad , \quad F_q^{1q1} = F_1^{q1q} = -1$$

Note that F_q^{qqq} coincides (up to a possible sign) with the Hadamard matrix. In any Ising theory, the clockwise monodromy of a pair of Ising anyons is given by

$$(3.3) \quad M^{qq} = \vartheta_q^{-2} \begin{pmatrix} \vartheta_0 & 0 \\ 0 & \vartheta_1 \end{pmatrix} = \vartheta_q^{-2} Z \quad , \quad Z = \begin{pmatrix} 1 & 0 \\ 0 & -1 \end{pmatrix}$$

That is, (up to a phase) the Pauli-Z matrix.²⁹

²⁹We know from Corollary 2.7(i) that $\varkappa_1 = 1$. It can be shown that any self-dual abelian anyon x with $\varkappa_x = 1$ has $\vartheta_x = \pm 1$. Then by the modularity of Ising theories, we must have $\vartheta_1 = -1$.

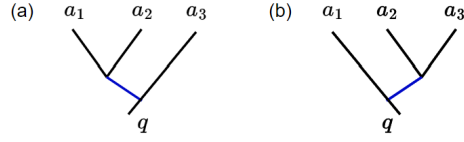


FIGURE 7. We can encode a qubit in the fusion space of 3 Ising anyons, $a_i = q$. The state evolution induced by the monodromy of (i) a_2, a_3 in fusion basis (a), or (ii) a_1, a_2 in basis (b), is given by (3.4), i.e. (up to a phase) the Pauli-X matrix.

$$(3.4) \quad F_q^{qqq}(M^{qq})^{\pm 1}F_q^{qqq} = \vartheta_q^{\mp 2}X$$

3.2. **One qubit.** We will break our analysis of the teleportation procedure into three phases, as highlighted between the horizontal dashed lines in Figure 8. Namely,

- (1) Initialisation and sharing of maximally entangled qubits, i.e. Charlie's operations.
- (2) Measurements and classical transmissions, i.e. Alice's operations.
- (3) *Correction step*, i.e. Bob's operations.

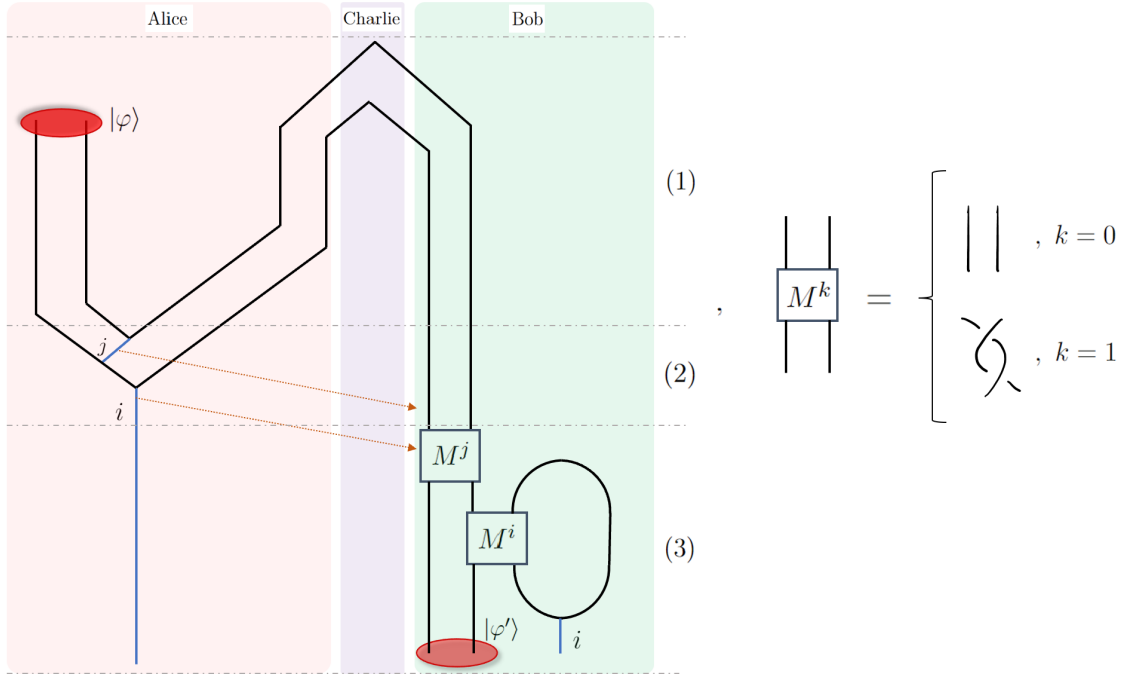
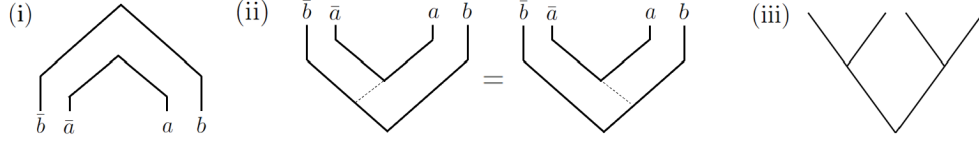


FIGURE 8. The 1-qubit teleportation protocol. Solid black worldlines represent Ising anyons, and solid blue worldlines represent anyons of charge 0 or 1. Dotted orange lines represent classical 1-bit transmissions from Alice to Bob. The final state $|\varphi'\rangle$ of Bob's pair of Ising anyons coincides (up to a global phase) with Alice's initial state $|\varphi\rangle$. For $i = 0$, the loop can be removed from the diagram.

Remark 3.2 (Freedom in procedure).

- (i) The distributor of the two pairs of Ising anyons is labelled Charlie (but could also just be either Alice or Bob).
- (ii) Fusion outcome j may instead be absorbed by Alice's rightmost remaining Ising anyon.
- (iii) The pair-creation and M_i -monodromy could be applied before the M_j -monodromy, and also to the left of Bob's Ising pair.
- (iv) The orientation of any monodromy applied by Bob does not matter.
- (v) Without loss of generality, we assume Alice to be to the left of Bob. Suppose their positions are swapped; then the teleportation procedure is given by viewing Figure 8 from behind.

3.2.1. *Charlie's operations.* Suppose Charlie is working with a system that supports some non-abelian anyons a and b such that $a \times b = \sum_c N_c^{ab} c$ where $N_c^{ab} = 0, 1$ for all c . Pair-creations of the form (i) below initialise fusion state (ii) in $V_0^{b\bar{a}ab}$; we will express this state in a basis of form (iii).



Let $d := \sum_c N_c^{ab}$. Since a and b are nonabelian, we know $d \geq 2$. Recoupling, we get

$$\begin{array}{c} \bar{b} \quad \bar{a} \quad a \quad b \\ \diagdown \quad \diagup \quad \diagdown \quad \diagup \\ \text{---} \quad \text{---} \quad \text{---} \quad \text{---} \\ \diagup \quad \diagdown \quad \diagup \quad \diagdown \\ \bar{b} \quad \bar{a} \quad a \quad b \end{array} = \sum_e [G_{\bar{b}}^{\bar{b}a\bar{a}}]_{e0} \begin{array}{c} \bar{b} \quad \bar{a} \quad a \quad b \\ \diagdown \quad \diagup \quad \diagdown \quad \diagup \\ \text{---} \quad \text{---} \quad \text{---} \quad \text{---} \\ \diagup \quad \diagdown \quad \diagup \quad \diagdown \\ \bar{b} \quad \bar{a} \quad a \quad b \end{array} = \sum_e [F_0^{eab}]_{\bar{e}\bar{b}} [G_{\bar{b}}^{\bar{b}a\bar{a}}]_{e0} \begin{array}{c} \bar{b} \quad \bar{a} \quad a \quad b \\ \diagdown \quad \diagup \quad \diagdown \quad \diagup \\ \text{---} \quad \text{---} \quad \text{---} \quad \text{---} \\ \diagup \quad \diagdown \quad \diagup \quad \diagdown \\ \bar{b} \quad \bar{a} \quad a \quad b \end{array} = \sum_e \eta_e |e\bar{e}\rangle =: |\psi\rangle$$

where $[F_0^{eab}]_{\bar{e}\bar{b}} \in U(1)$, and where $|[G_{\bar{b}}^{\bar{b}a\bar{a}}]_{e0}| = \sqrt{\frac{d_e}{d_a d_b}}$ by the unitarity of $L_e^{\bar{b}a}$. Suppose that all summands of $a \times b$ are abelian charges; then $|\eta_e| = d^{-1/2}$ for all e , which means that $|\psi\rangle$ is the state of two maximally entangled qudits (each with d logical basis states).

In the case of our Ising qubit teleportation (i.e. setting $a = b = q$), we see that Alice and Bob each possess one half of a Bell pair at the end of phase (1). The joint state of their systems at this juncture is $|\varphi\rangle |\psi\rangle \in V^{qq} \otimes V_0^{qqqq}$, where

$$(3.5) \quad |\varphi\rangle := \alpha |0\rangle + \beta |1\rangle$$

is Alice's qubit for teleportation, and Alice and Bob's shared Bell pair is

$$(3.6) \quad |\psi\rangle = \gamma |00\rangle + \delta |11\rangle, \quad \gamma := [G_q^{qqq}]_{00}, \quad \delta := [F_0^{1qq}]_{1q} [G_q^{qqq}]_{10}$$

3.2.2. *Alice's operations.* The state $|\varphi\rangle |\psi\rangle$ is in the initial basis shown in Figure 9. The leftmost pair of anyons encodes Alice's Ising qubit for teleportation, while the two rightmost pairs encode the maximally entangled qubits shared by Alice and Bob. We wish to transform to the final basis in Figure 9 in order to calculate the state of Bob's qubit after Alice makes her two measurements.

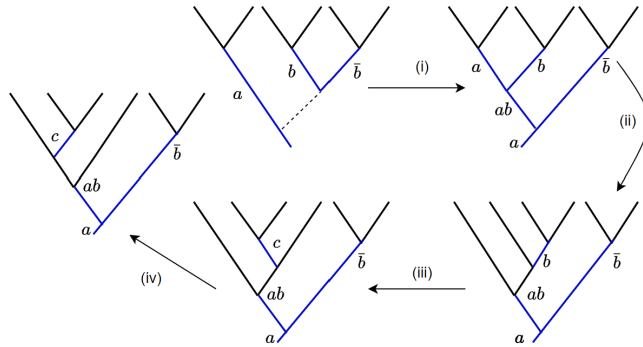


FIGURE 9. Solid black lines represent Ising anyons, and blue edges are labelled by $a, b, c \in \{0, 1\}$. In the above, ab denotes the fusion outcome of a and b . We have (i) $[G_a^{ab\bar{b}}]_{ab,0}$, (ii) $[F_{ab}^{qqb}]_{q,a}$, (iii) $\sum_c [G_q^{qqq}]_{c,b}$, (iv) $[G_{ab}^{qca}]_{q,q}$.

Let $g_{xy} = [G_q^{qqq}]_{xy}$ for all x, y . Expanding $|\varphi\rangle |\psi\rangle$ as per (3.6), we get

$$\alpha\gamma |000\rangle + \alpha\delta |011\rangle + \beta\gamma |100\rangle + \beta\delta |111\rangle$$

where basis kets have form $|a, b, \bar{b}\rangle$. Transformation (i) is trivial (in any gauge). Applying transformation (ii) yields

$$\alpha\gamma |000\rangle + \alpha\delta [F_1^{qq1}]_{q0} |111\rangle + \beta\gamma |100\rangle + \beta\delta [F_0^{qq1}]_{q1} |011\rangle$$

with basis kets of form $|ab, b, \bar{b}\rangle$. Finally, we apply (iii) to get

$$\begin{aligned} & \alpha\gamma(g_{00}|000\rangle + g_{10}|010\rangle) + \alpha\delta[F_1^{qq1}]_{q0}(g_{01}|101\rangle + g_{11}|111\rangle) \\ & + \beta\gamma(g_{00}|100\rangle + g_{10}|110\rangle) + \beta\delta[F_0^{qq1}]_{q1}(g_{01}|001\rangle + g_{11}|011\rangle) \end{aligned}$$

where basis kets take form $|ab, c, \bar{b}\rangle$. This can be rewritten as

$$(3.7) \quad \begin{aligned} & |00\rangle \left(\alpha\gamma g_{00}|0\rangle + \beta\delta[F_0^{qq1}]_{q1} \cdot g_{01}|1\rangle \right) + |01\rangle \left(\alpha\gamma g_{10}|0\rangle + \beta\delta[F_0^{qq1}]_{q1} \cdot g_{11}|1\rangle \right) \\ & + |10\rangle \left(\beta\gamma g_{00}|0\rangle + \alpha\delta[F_1^{qq1}]_{q0} \cdot g_{01}|1\rangle \right) + |11\rangle \left(\beta\gamma g_{10}|0\rangle + \alpha\delta[F_1^{qq1}]_{q0} \cdot g_{11}|1\rangle \right) \end{aligned}$$

Plugging in the values of the F -symbols gives

$$|00\rangle \left(\frac{\alpha}{2}|0\rangle + \frac{\beta}{2}|1\rangle \right) + |01\rangle \left(\frac{\alpha}{2}|0\rangle - \frac{\beta}{2}|1\rangle \right) + |10\rangle \left(\frac{\beta}{2}|0\rangle + \frac{\alpha}{2}|1\rangle \right) + |11\rangle \left(\frac{\beta}{2}|0\rangle - \frac{\alpha}{2}|1\rangle \right)$$

or more succinctly,

$$(3.8) \quad \frac{1}{2} \sum_{i,j \in \{0,1\}} |ij\rangle \otimes Z^j X^i |\varphi\rangle$$

That is, Alice measures outcome (i, j) with probability $\frac{1}{4}$, leaving Bob with state $Z^j X^i |\varphi\rangle$ at the end of phase (2) in Figure 8. Alice transmits her two measured bits to Bob over a classical channel, which concludes her operations.

Remark 3.3. If we apply the final transformation (iv) to the state (3.7), each tensor factor $|ab, c\rangle$ (where $ab, c = 0, 1$) evolves by a phase $[G_{ab}^{qqq}]_{q,q}$. Upon Alice's measurements, the contribution of such a phase to Bob's qubit is global. This verifies Remark 3.2(ii).

3.2.3. *Bob's operations.* It is clear from the above that Bob must apply a transformation $X^i Z^j$ to his qubit upon receipt of bits (i, j) from Alice. From (3.3), we know that a Z -correction is realised (up to a global phase) by a monodromy of his anyons. Let us verify that an X -correction is realised as shown in Figure 8.

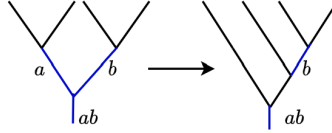


FIGURE 10. The leftmost pair of Ising anyons encode Bob's qubit, and the rightmost pair is ancillary. The change of basis shown is realised by $[F_{ab}^{qqb}]_{q,a}$.

Consider a basis state $|a, b, ab\rangle$ shown on the left-hand side of Figure 10, where $a, b \in \{0, 1\}$. The action by monodromy of the middle pair of anyons on this state is given in (3.9), where '+' denotes addition modulo 2: (i) is the change of basis in Figure 10; fixing the same gauge as in Section 3.1 and using (3.4), (ii) is the monodromy of the middle pair of anyons for this choice of fusion basis (up to an overall phase of $\vartheta_q^{\pm 2}$, which we discard); lastly, (iii) transforms back to the initial basis. We may remove 'ab' from the initial and final kets, since it is just the fusion product of the first two entries (and is thus redundant notation).

$$(3.9) \quad \begin{aligned} |a, b, ab\rangle & \xrightarrow{(i)} [F_{ab}^{qqb}]_{q,a} |b, ab\rangle \xrightarrow{(ii)} [F_{ab}^{qqb}]_{q,a} |b+1, ab\rangle \\ & \xrightarrow{(iii)} [G_{ab}^{qq(b+1)}]_{a+1,q} [F_{ab}^{qqb}]_{q,a} |a+1, b+1, ab\rangle \end{aligned}$$

Write the state of Bob's qubit for correction as $|\phi\rangle = \mu|0\rangle + \nu|1\rangle$. The ancillary pair is initialised from the vacuum, so $b = 0$. Following (3.9), the monodromy yields

$$(3.10) \quad |\phi\rangle|0\rangle = \mu|00\rangle + \nu|10\rangle \mapsto \mu[G_0^{qq1}]_{1q}[F_0^{qq0}]_{q0}|11\rangle + \nu[G_1^{qq1}]_{0q}[F_1^{qq0}]_{q1}|01\rangle$$

Plugging in the values of the F -symbols, that is $|\phi\rangle|0\rangle \mapsto X|\phi\rangle \otimes |1\rangle$. This concludes our verification.

3.3. Multiple qubits. Consider the process for teleporting the fusion state $|\varphi\rangle$ of Alice's $2p$ Ising anyons to Bob, as shown in Figure 11. Alice's measurements yield classical bits in order $z_p, x_p, \dots, z_1, x_1$, which she sequentially sends to Bob. The final state of Bob's Ising anyons coincides (up to a global phase) with Alice's initial state. Let us fix a fusion basis (3.11) for the state of the $2p$ Ising anyons. This has corresponding decomposition (3.12).

$$(3.11) \quad \begin{array}{cccc} 1 & 2 & \dots & 2p-1 & 2p \\ & \diagdown & & \diagup & \\ & & \dots & & \end{array}$$

$$(3.12) \quad V^{q^{\otimes 2p}} \cong \bigoplus_{k_1, \dots, k_p} V_{k_1}^{qq} \otimes \dots \otimes V_{k_p}^{qq} \otimes V^{k_1 \dots k_p} \cong \bigoplus_{k_1, \dots, k_p} V_{k_1}^{qq} \otimes \dots \otimes V_{k_p}^{qq}$$

However, note that (3.11) does not fully specify a fusion basis. Nonetheless, we see from the corresponding decomposition (3.12) that it effectively does so. This is since, (a) each space $V^{k_1 \dots k_p}$ is 1-dimensional, whence the second isomorphism in (3.12) holds; (b) a change of basis transformation between any two decompositions of a space $V^{k_1 \dots k_p}$ is trivial (in any gauge). We may thus write

$$(3.13) \quad |\varphi\rangle = \sum_{k \in \mathbb{Z}_2^p} \alpha_k |k\rangle \quad , \quad k = k_1 \dots k_p \quad , \quad \text{i.e.} \quad |k\rangle = |k_1\rangle \dots |k_p\rangle \quad , \quad k_i \in \mathbb{Z}_2$$

where $\sum_k |\alpha_k|^2 = 1$. This tells us that the fusion state of $2p$ Ising anyons can encode p qubits of information. From Figure 11, we see that if Alice and Bob share p ebits³⁰, they can teleport (at most) the state of $2p + 1$ Ising anyons.³¹

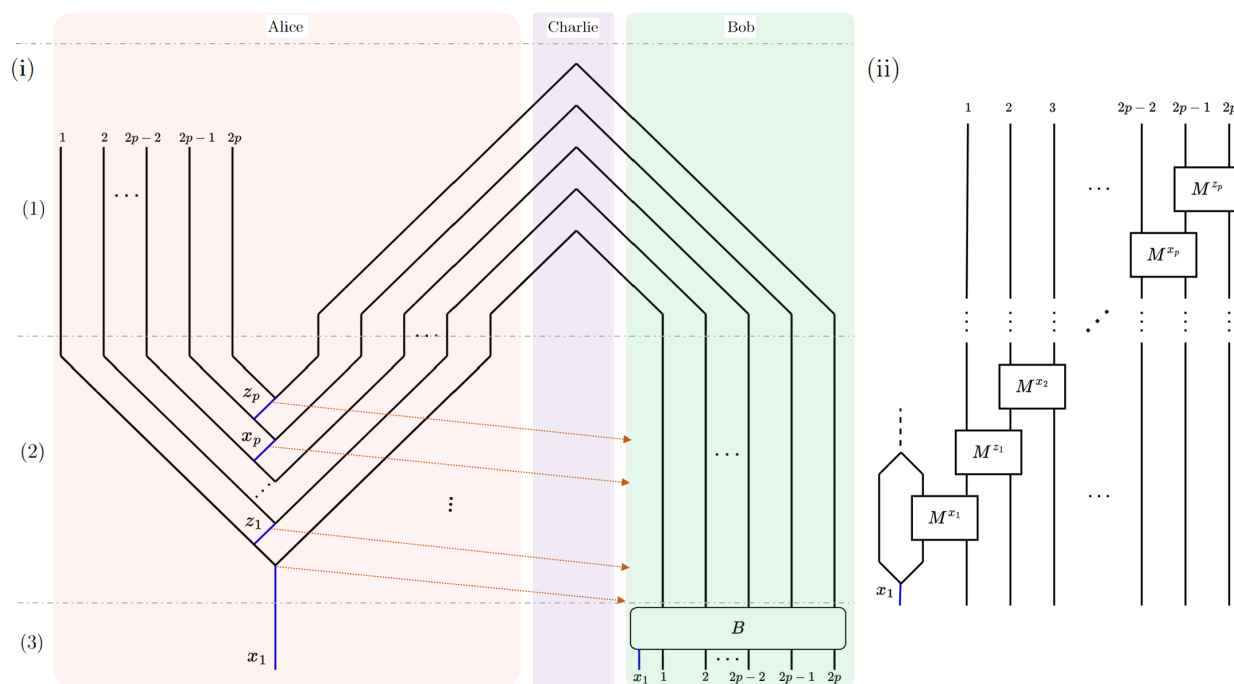


FIGURE 11. (i) The multi-qubit teleportation protocol, $p \geq 2$. Solid black worldlines represent Ising anyons, and solid blue worldlines represent anyons of charge 0 or 1. Dotted orange lines represent classical 1-bit transmissions from Alice to Bob. The coupon $B = B(x_1, z_1, \dots, x_p, z_p)$ represents Bob's *correction step*, and is shown in (ii) (where coupons ' M ' are defined as in Figure 8).

³⁰Recall from Section 3.2.1 that 1 ebit is encoded in the fusion state of two pairs of Ising anyons here (where each pair encodes a maximally entangled qubit).

³¹Note that $V^{q^{\otimes (2p+1)}} \cong V^{q^{\otimes 2p}}$ for $p \geq 1$. That is, given an collection of N Ising anyons for N odd, we can discard one of the outermost anyons without affecting the encoded fusion state. Thus, the fusion state of N Ising anyons can encode $\lfloor \frac{N}{2} \rfloor$ qubits of information. For this reason, we take $N = 2p$ in our discussion.

As with the single-qubit case, we split our analysis of the protocol into phases (1)-(3) as delineated by the horizontal dashed lines in Figure 11. At the end of phase (1), the joint state of the $6p$ Ising anyons is $|\varphi\rangle \otimes \bigotimes_{i=1}^p |\psi_i\rangle$, where $|\psi_i\rangle$ is the Bell state $|\psi\rangle$ (as given in (3.6)) for each i .

$$V^{q^{\otimes 6p}} \cong V^{q^{\otimes 2p}} \otimes \left(\bigoplus_{l_1, \dots, l_p} V_{l_1}^{qq} \otimes \dots \otimes V_{l_p}^{qq} \otimes V_{l_p}^{qq} \otimes \dots \otimes V_{l_1}^{qq} \right), \quad |\psi_i\rangle \in \bigoplus_{l_i \in \mathbb{Z}_2} V_{l_i}^{qq} \otimes V_{l_i}^{qq}$$

In order to determine the state of Bob's $2p$ anyons at the end of phase (2), we will combine the first two phases and shift our perspective to the one shown in Figure 12. In Figure 11, the p ebits are generated before Alice's measurements (i.e. they can be preshared); whereas in Figure 12, creation and sharing of ebits alternates with Alice's measurements.

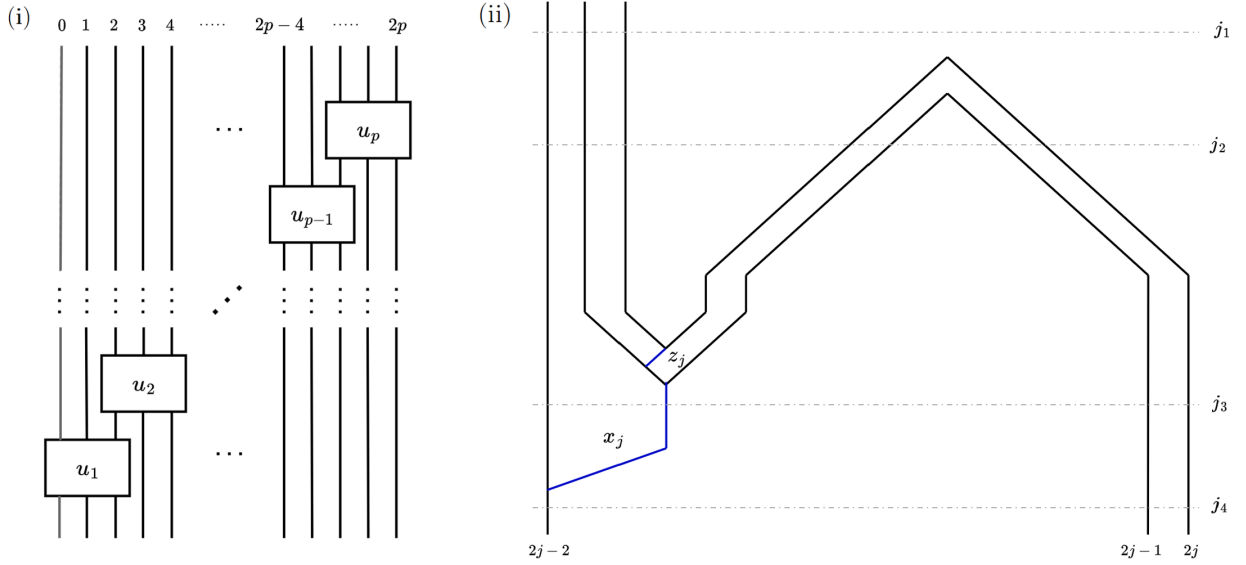


FIGURE 12. We take the subdiagram for phases (1)-(2) in Figure 11, and apply a planar isotopy (without rotating any trivalent vertices) to arrive at the physically equivalent process shown in (i). The line enumerated by 0 represents the vacuum, and the morphism represented by coupon u_j is given in (ii).

Let $|\varphi_{j,a}\rangle$ denote the state of all Ising anyons across the system at instant j_a of the process shown in Figure 12. States $|\varphi_{j,a}\rangle$ are realised in temporal order j_1, \dots, j_4 for $j = p$ to 1. Note that (i) $|\varphi_{p,1}\rangle = |\varphi\rangle$; (ii) each $|\varphi_{j,a}\rangle$ is the state of $2p$ Ising anyons, save for $a = 2$ where it is the state of $2p + 4$ Ising anyons. At the end of phases (1)-(2), Bob is left with $2p$ Ising anyons in state $|\varphi_{1,4}\rangle$ which we will now calculate in the primed basis (3.11). We say that the p^{th} qubit is encoded in the fusion space of the Ising anyons enumerated $2p - 1$ and $2p$.

- (j_1) : $|\varphi_{j,1}\rangle = |\varphi_{j+1,4}\rangle$ for $j < p$
- (j_2) : $|\varphi_{j,2}\rangle = |\varphi_{j,1}\rangle |\psi\rangle \in V^{q^{\otimes 2p}} \otimes \left(\bigoplus_{e \in \{0,1\}} V_e^{qq} \otimes V_e^{qq} \right)$ where $|\psi\rangle$ is the Bell state (3.6).
- (j_3) : $|\varphi_{j,3}\rangle = 2B_j X_j^{x_j} |\varphi_{j,1}\rangle$ where $X_j := \bigotimes_{n=1}^p X^{\delta_{nj}}$, $B_j := \bigotimes_{n=1}^p B(x_j, z_j)^{\delta_{nj}}$ and

$$B(x_j, z_j) := \begin{pmatrix} \gamma \cdot g_{z_j,0} & 0 \\ 0 & \delta \cdot [F_{x_j}^{qq1}]_{q, x_j+1} \cdot g_{z_j,1} \end{pmatrix}$$

Note that $x_j + 1$ is modulo 2 and that $2B_j$ is unitary. Measurement outcomes (x_j, z_j) are uniformly distributed. This follows from our 1-qubit analysis (see (3.7)).

(j_4) : For $j = 1$, we have $|\varphi_{1,4}\rangle = |\varphi_{1,3}\rangle$. For $j > 1$,

$$\begin{array}{c} 2j-3 \quad 2j-2 \quad x_j \\ \diagdown \quad \diagup \\ b \\ \diagup \quad \diagdown \\ b+x_j \end{array} = [F_{b+x_j}^{qqx_j}]_{qb} \begin{array}{c} 2j-3 \quad 2j-2 \quad x_j \\ \diagdown \quad \diagup \\ \dots j_4 \\ \diagup \quad \diagdown \\ b+x_j \end{array}$$

where $b+x_j$ is modulo 2. The $(2j-2)^{th}$ Ising anyon absorbs an anyon of charge x_j . Note that Alice's $(j-1)^{th}$ qubit is bit-flipped when $x_j = 1$. More precisely,

$$|\varphi_{j,4}\rangle = \tilde{X}_{j-1}^{x_j} |\varphi_{j,3}\rangle, \quad \tilde{X}_j := \bigotimes_{n=1}^p \tilde{X}^{\delta_{nj}} \quad \text{where} \quad \tilde{X} := \begin{pmatrix} 0 & [F_0^{qq1}]_{q1} \\ [F_1^{qq1}]_{q0} & 0 \end{pmatrix}$$

Thus, at the start of phase (3) in Figure 11, Bob's $2p$ Ising anyons are in fusion state

$$(3.14) \quad |\varphi_{1,4}\rangle = \sum_{k \in \mathbb{Z}_2^p} \alpha_k \left[\left(2B(x_1, z_1) X^{x_1} \tilde{X}^{x_2} |k_1\rangle \right) \otimes \dots \otimes \left(2B(x_{p-1}, z_{p-1}) X^{x_{p-1}} \tilde{X}^{x_p} |k_{p-1}\rangle \right) \right. \\ \left. \otimes \left(2B(x_p, z_p) X^{x_p} |k_p\rangle \right) \right]$$

Fixing the same gauge as in Section 3.1 and plugging in the F -symbols, (i) \tilde{X} coincides with X ; and, (ii) $2B(x_j, z_j)$ coincides with $|0\rangle\langle 0| + (-1)^{z_j} |1\rangle\langle 1| = Z^{z_j}$. Thus,

$$(3.15) \quad |\varphi_{1,4}\rangle = \sum_k \alpha_k \left(\bigotimes_{j=1}^p Z^{z_j} X^{x_j+x_{j+1}} |k_j\rangle \right) = \left(\bigotimes_{j=1}^p Z^{z_j} X^{x_j+x_{j+1}} \right) |\varphi\rangle, \quad x_{p+1} := 0$$

where $x_j + x_{j+1}$ is modulo 2. This state is obtained with probability 4^{-p} .

3.3.1. Correction step. We now consider the operations that Bob performs on his $2p$ Ising anyons in order to recover Alice's initial fusion state $|\varphi\rangle$. We continue to work in the gauge from Section 3.1. The Z -errors are corrected via braid $\prod_{j=1}^p \sigma_{2j-1}^{\pm 2z_j}$ which realises (up to a global phase) the operator $\bigotimes_{j=1}^p Z^{z_j}$ (in any gauge). This leaves Bob with the state $|\varphi''\rangle := \bigotimes_{j=1}^p X^{x_j+x_{j+1}} |\varphi\rangle$. We introduce a toy model (Figure 13) so as to clearly understand the relationship between the state $|\varphi''\rangle$ and Alice's measurement outcomes (x_1, \dots, x_p) .

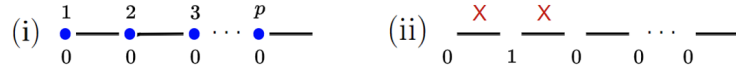


FIGURE 13. (i) Vertices (blue dots) are enumerated from 1 to p . The j^{th} vertex has the value x_j directly beneath, and lies on the left-side of the j^{th} edge. The j^{th} edge represents the j^{th} qubit. When $x_j = 0$ for all j , the graph represents state $|\varphi\rangle$. (ii) We shall henceforth typically omit the enumerated vertices. When the j^{th} vertex changes value (i.e. x_j flips), a bit-flip is applied to the adjacent edges. This is described by the action of ‘vertex operator’ $v_j := X_{j-1} X_j$.¹ This graph corresponds to the state $v_2 |\varphi\rangle$, which has two X -errors (i.e. bit-flip errors) relative to the state $|\varphi\rangle$ at ‘sites’ (i.e. edges or qubits) 1 and 2. An X -error on the j^{th} qubit is represented by a red cross at the j^{th} site.

¹ X_0 can be thought of as a Pauli- X operator acting on a fictitious site (or indeed, a physical ancillary site as introduced below) numbered 0 at the left boundary.

Since the diagram representing a state is drawn as sites occupied by either nothing (‘nought’) or crosses, we call the toy model the *noughts and crosses model*, or $\text{O}\times$ -model for short. Let $\hat{x}_j := v_j^{x_j}$. Note that $|\varphi''\rangle = \hat{x}_1 \dots \hat{x}_p |\varphi\rangle$. In (3.16), we consider the action of the self-inverse operator v_j on sites j and $j-1$ for $j \geq 2$.

$$(3.16) \quad v_j \left(\begin{array}{c} \times \quad \times \\ _ \quad _ \end{array} \right) = \left(_ \quad _ \right), \quad v_j \left(\begin{array}{c} _ \quad \times \\ _ \quad _ \end{array} \right) = \left(\times \quad _ \right)$$

That is, v_j can pair-create and annihilate X -errors, or propagate an X -error. In the context of Alice's generation of Bob's state $|\varphi''\rangle$, we consider the action of time-ordered (i.e. right-to-left) operator $\hat{x}_1 \dots \hat{x}_p$ on $|\varphi\rangle$.³² Commencing at the p^{th} site and moving leftward with each step, any possible accumulation of X -errors will occur as follows.

- (1) (i) A pair-creation of X -errors, possibly followed by (ii) leftward propagation of the leftmost X -error. Then possibly loop back to (i).
- (2) Finally, if $x_1 = 1$ then the total number of X -errors must be odd and we call the leftmost error an *edge-error*. Such an error can arise in two ways: (a) if $x_2 = 1$ then in the final iteration of (1), the leftmost X -error has been propagated all the way 'out' of the system of qubits; (b) if $x_2 = 0$, the edge-error does not come from a pair-creation and has been generated through the action of v_1 alone.

Of course, (1) or (2) may not occur at all. It follows that X -errors come in pairs with the exception of a possible edge-error. Given a binary string $x_1 \dots x_p$, we can determine the OX -diagram for $|\varphi''\rangle$ using the following observation: any substring of 1s gives rise to one of the following two cases (which respectively correspond to (1)-(2) above).

- (1) For $j > 1$ and $l \geq 0$, a substring $x_j \dots x_{j+l}$ of 1s such that (i) $x_{j-1} = 0$, and (ii) $x_{j+l+1} = 0$ or $j+l = p$. The corresponding OX -subdiagram for $|\varphi''\rangle$ has crosses at sites $j-1$ and $j+l$, and nothing at any sites in between.

$$(3.17) \quad \begin{array}{cccccc} & j-1 & & j & & j+1 & & j+l-1 & & j+l \\ & & & \times & & & & & & \times \\ & & & \text{---} & & \dots & & \text{---} & & \\ 0 & & & 1 & & 1 & & 1 & & 1 \end{array}$$

- (2) For $j \geq 1$, a substring $x_1 \dots x_j$ of 1s such that $x_{j+1} = 0$ or $j = p$. The corresponding OX -subdiagram for $|\varphi''\rangle$ has a cross at the j^{th} site, and nothing at any preceding sites.

$$(3.18) \quad \begin{array}{cccc} & 1 & & 2 & & j-1 & & j \\ & & & & & & & \times \\ & & & \text{---} & & \dots & & \text{---} \\ 1 & & & 1 & & 1 & & 1 \end{array}$$

Example 3.4. A tabulation of all possible OX -diagrams for $|\varphi''\rangle$ when $p = 4$. Note the presence of an edge-error in the final two columns.

0 --- 0 --- 0 --- 0 ---	0 --- \times --- 1 --- \times --- 0 --- 0 ---	1 --- \times --- 0 --- 0 --- 0 ---	1 --- \times --- 1 --- 0 --- 0 ---
0 --- 0 --- 0 --- \times --- \times ---	0 --- \times --- 1 --- \times --- 0 --- 1 --- \times ---	1 --- \times --- 0 --- 0 --- 1 --- \times ---	1 --- 1 --- \times --- \times --- \times ---
0 --- 0 --- \times --- 1 --- \times --- 0 ---	0 --- \times --- 1 --- 1 --- \times --- 0 ---	1 --- \times --- 0 --- \times --- 1 --- \times --- 0 ---	1 --- 1 --- 1 --- \times --- 0 ---
0 --- 0 --- \times --- 1 --- 1 --- \times ---	0 --- \times --- 1 --- 1 --- 1 --- \times ---	1 --- \times --- 0 --- \times --- 1 --- 1 --- \times ---	1 --- 1 --- 1 --- 1 --- \times ---

Vertex operators via braiding. We can realise the operators $\{v_j\}_{j=2}^p$ through a monodromy of the Ising anyons enumerated $2j-2$ and $2j-1$. This follows from the discussion in Section 3.2.3. Specifically, by (3.9) we have that the monodromy induces transformations

$$|00\rangle \mapsto [G_0^{qq1}]_{1q} |11\rangle \quad , \quad |01\rangle \mapsto [F_1^{qq1}]_{q0} |10\rangle \quad , \quad |10\rangle \mapsto [G_1^{qq1}]_{0q} |01\rangle \quad , \quad |11\rangle \mapsto [F_0^{qq1}]_{q1} |00\rangle$$

up to some global phase, where the left-hand side of each transformation represents the components of the $(j-1)^{\text{th}}$ and j^{th} qubits in the p -qubit state.

³²We specify time-ordering here, since $[\hat{x}_i, \hat{x}_j] = 0$.

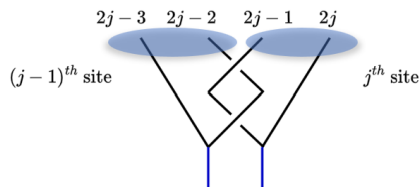


FIGURE 14. The monodromy realises the operator $X_{j-1}X_j = v_j$.

What of v_1 ? On either the left or right boundary of Bob's $2p$ Ising anyons, he can initialise an additional pair from the vacuum, enumerated $(-1, 0)$ and $(2p + 1, 2p + 2)$ respectively. This corresponds to an ancillary qubit in state $|0\rangle$ at ancillary sites enumerated 0 and $p + 1$ respectively. Then by the above, we have that

- (a) A monodromy of anyons 0 and 1 flips the state of both the 1^{st} qubit and left ancilla (i.e. 0^{th} qubit). This realises $v_1 = (X_0 \otimes)X_1$.
- (b) A monodromy of anyons $2p$ and $2p + 1$ flips the state of both the p^{th} qubit and right ancilla (i.e. $(p + 1)^{th}$ qubit). This realises $X_p(\otimes X_{p+1}) =: v_{p+1}$.

Parenthesised operators emphasise that their action is on ancillaries. In this way, we can introduce or remove an X -error at the first and last of the p sites. Note that we corrected X -errors this way in the 1-qubit case (e.g. (b) appears in Figure 8).

Commutativity and braidwords. Let $\rho : \text{PB}_{2p+2} \rightarrow \text{U}(2^{p+2})$ be the unitary linear (pure) braid representation arising from our system of p qubits and two ancillary qubits (along with our choice of fusion basis and gauge). We enumerate our $2p + 2$ -strand pure braid generators $\{\sigma_i^{\pm 2}\}_{i=0}^{2p}$. Specifically, the generators have image (up to a global phase which we can ignore) given by

$$(3.19) \quad \rho(\sigma_{2i}^{\pm 2}) = v_{i+1} = X_i X_{i+1} \quad , \quad \rho(\sigma_{2j-1}^{\pm 2}) = Z_j \quad , \quad 0 \leq i \leq p \quad , \quad 1 \leq j \leq p$$

For $s, t \in \{-1, 1\}$, we have that $\rho(\sigma_k^{2s}), \rho(\sigma_l^{2t})$ commute for all k, l such that $|k - l| \neq 1$; they anticommute when $|k - l| = 1$, yet effectively commute since the sign physically amounts to a global phase factor. We henceforth take ρ as implicit when considering the braid action.

Remark 3.5. Whenever operators $v_1 = \sigma_0^{\pm 2}$ (equivalently \hat{x}_1 for $x_1 = 1$) or $v_{p+1} = \sigma_{2p}^{\pm 2}$ appear, we implicitly assume that they have been respectively preceded by at least one pair-creation operator acting at the left and right boundaries. Explicitly, given p -qubit state $|\Psi\rangle$ we can respectively write these left and right pair-creation operators as

$$a_l^\dagger : |\Psi\rangle \mapsto |0\rangle |\Psi\rangle \quad , \quad a_r^\dagger : |\Psi\rangle \mapsto |\Psi\rangle |0\rangle$$

Freedom in eradication of X -errors. We have seen that the removal of X -errors is realised via pair-annihilations over the p sites, possibly combined with the addition or removal of X errors at boundaries.³³ Given $|\varphi''\rangle$, there are typically several distinct ways to do so. For instance, when $(x_1, x_2, x_3, x_4) = (0, 0, 1, 1)$ in Example 3.4, this can be achieved, e.g. via (i) $\hat{x}_4 \hat{x}_3 = v_4 v_3$, or (ii) $v_5 v_2 v_1$. Of course, we may in turn reorder the operators in each of these solutions.

It may be the case that a solution is selected with respect to constraints such as minimising the number of monodromies employed (especially for p large) or pair-creations at boundaries. In the presence of an edge error, there may also be a preference as to on which side the net charge of ‘1’ is left. With any number of these requirements in mind, the correction of X -errors reduces to an optimisation problem. We do not address this issue here, but instead provide a generic prescription that works in any case.

Generic prescription for error-correction. Recall that Alice's measurements yield classical bits in order $z_p, x_p, \dots, z_1, x_1$ (which she sequentially sends to Bob), and that $\hat{x}_j = v_j^{x_j}$. We further

³³Ancillary anyons can be fused together at each boundary. It can be seen that if $|\varphi''\rangle$ contains an edge error, any possible elimination of X -errors will result in a net topological charge of ‘1’ across the the left and right boundaries of Bob's $2p$ Ising anyons; else, this net charge will always be trivial.

define operator $\hat{z}_j = (Z_j)^{z_j}$, whence we have $\{\hat{x}_j, \hat{z}_j\}_{j=1}^p$. Then for any possible $|\varphi_{1,4}\rangle$ (the p -qubit fusion state of Bob's $2p$ Ising anyons at the start of phase (3)), we have that

$$(3.20) \quad (\hat{x}_1 \cdots \hat{x}_p)(\hat{z}_1 \cdots \hat{z}_p) |\varphi_{1,4}\rangle = |\varphi\rangle \quad , \quad \hat{x}_j = \sigma_{2j-2}^{\pm 2x_j} \quad , \quad \hat{z}_j = \sigma_{2j-1}^{\pm 2z_j}$$

The operator $\hat{x}_1 \cdots \hat{x}_p$ can be interpreted as a repetition of steps (1)-(3) below until all p sites are free from X -errors.

- (1) Take the rightmost X -error (if any exist) at site j .
- (2) Propagate it leftwards until it reaches site j' such that either (a) $j' - 1$ is occupied by an X -error, or (b) $j' = 1$ (in which case it is an edge error).³⁴
- (3) Immediately following instance (a) the X -errors then pair-annihilate. Immediately following instance (b) the X -error is propagated 'out' of the system (onto ancillary site 0) and the correction is complete.

In any gauge, the correction operator $(\hat{x}_1 \cdots \hat{x}_p)(\hat{z}_1 \cdots \hat{z}_p)$ in (3.20) coincides (up to a global phase) with the correction operator B from Figure 11(ii) (i.e. we have the freedom to slide coupons past one another). This proves Theorem 3.1.

Remark 3.6. While prescription (3.20) is a catch-all, there are scenarios in which it may be grossly inefficient, e.g. for p large,

- (i) Two X -errors at sites r, s (with none in-between them and $r < s$) where $p - (s - r)$ is small. Suppose the the generic prescription would pair-annihilate them. It would be more efficient to remove them by instead propagating errors at sites r and s respectively left and right.
- (ii) An edge-error at site r where $p - r$ is small. It is more efficient to propagate this 'out' of the system from the right boundary.

4. SUPERDENSE CODING OF BITS BY BRAIDING ISING ANYONS

The goal of this section is to prove the following theorem.

Theorem 4.1. *We can realise the superdense coding protocol using Ising anyons, as shown in Figure 15. In particular, braiding is not required anywhere other than the 2-bit encoding step.*

We will break our analysis of the superdense coding procedure into three phases, as highlighted between the horizontal dashed lines in Figure 15. Namely,

- (1) Initialisation and sharing of maximally entangled qubits, i.e. Charlie's operations.
- (2) Encoding of bits $i, j \in \mathbb{Z}_2$ and transmission of qubit, i.e. Alice's operations.
- (3) Measurements and recovery of bits i, j , i.e. Bob's operations.

Remark 4.2 (Relation to teleportation). Recall that the superdense coding and teleportation protocols are 'dual' in some sense. Compare the process for superdense coding in Figure 15 to the one for teleportation in Figure 8. Altogether, the phases of the latter correspond to a composition of operations $\mathcal{O}_3 \circ (\mathcal{O}_2 \otimes \text{id}) \circ (\text{id} \otimes \mathcal{O}_1)$ where (a) id is a 1-qubit operator; (b) \mathcal{O}_1 creates two (maximally entangled) qubits; (c) \mathcal{O}_2 measures two qubits (in a specified fusion basis); (d) \mathcal{O}_3 is a unitary 1-qubit operator (conditioned on i, j)³⁵. The former is given by $\mathcal{O}_2 \circ (\text{id} \otimes \mathcal{O}_3) \circ \mathcal{O}_1$. The analysis of the superdense coding procedure is thus largely the same. The highlighted relationship is perhaps unsurprising, as it can be analogously observed in the quantum circuit formulation of both protocols.

³⁴Of course, if $j' = j$ then no propagation is necessary.

³⁵For $i = 1$, \mathcal{O}_2 is a 2-qubit operator if we additionally count the bit-flip action on the ancillary qubit.

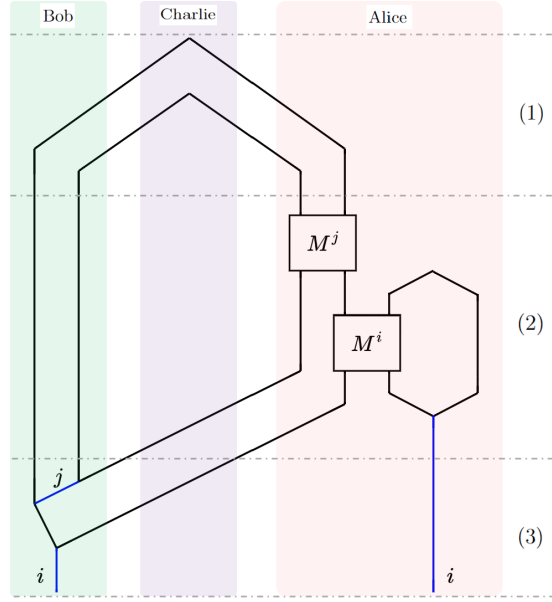


FIGURE 15. Superdense coding protocol using Ising anyons. Alice and Bob have maximally entangled Ising qubits. Alice encodes bits i, j in her qubit, which she then sends to Bob who is able to recover the bits by measurement. Solid black worldlines represent Ising anyons, and solid blue worldlines represent anyons of charge 0 or 1. Coupons M^i, M^j are as in Figure 8. For $i = 0$, the rightmost loop can be omitted.

Charlie's operations. The analysis is identical to that in Section 3.2.1, and shows that Alice and Bob share a Bell pair $|\psi\rangle \in V_0^{qqqq}$ at the end of phase (1). State $|\psi\rangle$ is given precisely in (3.6), which in our choice of gauge, can be written $\frac{1}{\sqrt{2}}(|00\rangle + |11\rangle)$. Basis kets have form $|a, b\rangle$ in correspondence with the leftmost fusion basis of Figure 16.³⁶

Alice's operations. The analysis here is identical to that of Section 3.2.3. Coupons M^j and M^i respectively correspond to the action of operators Z^j and X^i on Alice's half of the Bell pair. So we have state evolution (4.1) where ' $k + i$ ' is modulo 2.

$$(4.1) \quad \frac{1}{\sqrt{2}} \sum_{k \in \mathbb{Z}_2} |kk\rangle \xrightarrow{M^j} \frac{1}{\sqrt{2}} \sum_k (-1)^{jk} |kk\rangle \xrightarrow{M^i} \frac{1}{\sqrt{2}} \sum_k (-1)^{jk} |k, k+i\rangle =: |\psi'\rangle$$

In particular, $M^i : V_0^{qqqq} \rightarrow V_i^{qqqq}$. The 2-qubit state at the end of phase (2) is $|\psi'\rangle \otimes |i\rangle$ when expressed with respect to basis kets of form $|a, b, ab\rangle$ (for the leftmost fusion basis of Figure 16).

Bob's operations. Bob receives Alice's qubit and is now in possession of 2-qubit state $|\psi'\rangle$. He measures this state in the rightmost fusion basis of Figure 16.

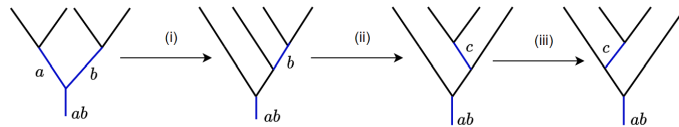


FIGURE 16. Blue edges are labelled by $a, b, c \in \{0, 1\}$. Here, ab denotes the fusion outcome of a and b . We have (i) $[F_{ab}^{qqb}]_{q,a}$, (ii) $\sum_c [G_q^{qqq}]_{c,b}$, (iii) $[G_{ab}^{qcq}]_{q,q}$. These transformations are contained in Figure 9, but we include them here for convenience.

³⁶ $|a, b\rangle$ is shorthand for $|a, b, ab\rangle$.

Applying change of basis transformations (i)-(iii),

$$\begin{aligned}
 |\psi'\rangle |i\rangle &\xrightarrow{(i)} \left(\frac{1}{\sqrt{2}} \sum_k (-1)^{jk} [F_i^{q,q,k+i}]_{qk} |k+i\rangle \right) \otimes |i\rangle \xrightarrow{(ii)} \left(\frac{1}{\sqrt{2}} \sum_{k,l} (-1)^{jk} [G_q^{qqq}]_{l,k+i} [F_i^{q,q,k+i}]_{qk} |l\rangle \right) \otimes |i\rangle \\
 &\xrightarrow{(iii)} \left(\frac{1}{\sqrt{2}} \sum_{k,l} (-1)^{jk} [G_i^{qlq}]_{qq} [G_q^{qqq}]_{l,k+i} [F_i^{q,q,k+i}]_{qk} |l\rangle \right) \otimes |i\rangle
 \end{aligned}$$

By (3.2), we have $[G_i^{qlq}]_{qq} = (-1)^{il}$, $[G_q^{qqq}]_{l,k+i} = (-1)^{l(k+i)}/\sqrt{2}$, $[F_i^{q,q,k+i}]_{qk} = 1$ where any addition in indices or exponents is modulo 2. Plugging these in gives

$$\frac{1}{2} \sum_{k,l} (-1)^{(j+l)k} |l\rangle |i\rangle = \frac{1}{2} [(1 + (-1)^j) |0\rangle + (1 - (-1)^j) |1\rangle] \otimes |i\rangle = |j\rangle |i\rangle$$

whence we see that Bob successfully recovers Alice's bits.³⁷ This proves Theorem 4.1.

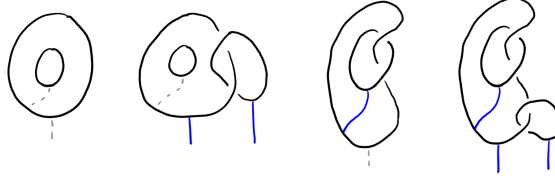


FIGURE 17. From left to right: superdense coding processes for $ij = 00, 10, 01, 11$ respectively. A solid blue worldline represents an anyon of charge 1 here.

5. QUDIT TELEPORTATION AND d -ARY SUPERDENSE CODING WITHOUT BRAIDING

We now generalise the protocols of Sections 3 and 4 to a d -ary setting for $d \geq 2$ (with some caveats regarding d discussed in Section 5.1 below). Moreover, we remove the need for any braiding. We use the term *dit* for the d -ary generalisation of a bit, and (analogously to an ebit) we use *e-dit* to refer to a maximally entangled pair of qudits.

The results of this section pertain to Tambara-Yamagami theories, introduced in Section 5.1. These include Ising theories as a special case. We proceed to construct a braid-free qudit teleportation procedure in Section 5.2, where the primary objective is to prove the following theorem.

Theorem 5.1. *Consider a Tambara-Yamagami theory of rank $d+1$ where $d = 2^n$. The fusion state of N Tambara-Yamagami anyons (that is, an $N/2$ -qudit state, where N is even) can be teleported via the procedure shown in Figure 18. In particular, no braiding is required.*

In Section 5.2.1, we establish supporting results that are required for the proof of this theorem. The proof rests on Lemma 5.7, alongside the simple observation labelled as Lemma 5.6. A short digression is found in Section 5.2.2, where we see that the teleportation protocol finds an obvious interpretation in the graphical calculus. In Section 5.2.3, we show that the braidless teleportation procedure works as claimed, i.e. we prove Theorem 5.1. The discourse of Section 5.2.1 also gives rise to the following theorem.

Theorem 5.2. *We can apply Pauli gates to an Ising qubit without braiding. The (braid-free) Pauli gates $\{I, X, Y, Z\}$ are realised by U_{g_1, g_2} as defined in equation (5.1), for $g_1, g_2 \in \mathbb{Z}_2$.*

$$(5.1) \quad U_{g_1, g_2} \in \left[\begin{array}{c} \text{---} \\ \text{---} \\ \text{---} \\ \text{---} \\ \text{---} \\ \text{---} \\ \text{---} \end{array} \right] \in \left[\begin{array}{c} \begin{array}{c} \text{---} \\ \text{---} \\ \text{---} \\ \text{---} \\ \text{---} \\ \text{---} \\ \text{---} \end{array} \\ \begin{array}{c} \text{---} \\ \text{---} \\ \text{---} \\ \text{---} \\ \text{---} \\ \text{---} \\ \text{---} \end{array} \end{array} \right], \quad g_j \in \left[\begin{array}{c} \text{---} \\ \text{---} \\ \text{---} \\ \text{---} \\ \text{---} \\ \text{---} \\ \text{---} \end{array} \right] \in \left[\begin{array}{c} \begin{array}{c} \text{---} \\ \text{---} \\ \text{---} \\ \text{---} \\ \text{---} \\ \text{---} \\ \text{---} \end{array} \\ \begin{array}{c} \text{---} \\ \text{---} \\ \text{---} \\ \text{---} \\ \text{---} \\ \text{---} \\ \text{---} \end{array} \end{array} \right]$$

³⁷Note that Bob can alternatively fuse charge j with the Ising anyon on the right in Figure 15. This is seen by applying transformations (i)-(ii) to $|\psi'\rangle$, yielding $(-1)^{ij} |j\rangle |i\rangle$. As per Remark 3.2(ii), the same freedom appears in the qubit teleportation procedure, as expected by the duality of the protocols.

In (5.1), we follow our usual convention, where solid black lines represent Ising anyons, and solid blue worldlines represent abelian anyons with charge 0 or 1.

Finally, in Section 5.3, we construct a braid-free d -ary superdense coding procedure. That is, we prove the following theorem.

Theorem 5.3. *Consider a Tambara-Yamagami theory of rank $d + 1$ where $d = 2^n$. We can realise the d -ary superdense coding protocol using Tambara-Yamagami anyons, as shown in Figure 22(i). In particular, braiding is not required anywhere other than the 2-dit encoding step.*

5.1. Tambara-Yamagami anyons. Let G be a finite abelian group of order $d \geq 2$. Consider labels $\{q\} \cup \{g\}_{g \in G}$ with fusion rules (5.2); ‘ \cdot ’ is the group operation of G (henceforth omitted).

$$(5.2) \quad q \times q = \sum_{g \in G} g, \quad q \times g = g \times q = q, \quad g \times g' = g \cdot g'$$

Fusion rules of the form (5.2) always give rise to a fusion category [28]; any such category is called *Tambara-Yamagami* and is denoted by $\text{TY}(G)$. Furthermore, any fusion category $\text{TY}(G)$ is unitary: this follows from [29, Theorem 5.20], since $\text{TY}(G)$ weakly group-theoretical.³⁸

Remark 5.4 (Physical realisability). If $\text{TY}(G)$ admits a braiding, then it should be realisable as a theory of anyons.³⁹ Indeed, this is the case for $d = 2$, i.e. $\text{TY}(\mathbb{Z}_2)$ (this corresponds to the ‘Ising theories’ of Section 3.1, all of which are modular). In fact, $\text{TY}(G)$ admits a braiding if and only if $G \cong \mathbb{Z}_2^n$ for all $n \geq 1$ [12, Theorem 1.2 (1)]. We shall thus assume $G \cong \mathbb{Z}_2^n$ (consequently, $d = 2^n$) in the following, unless stated otherwise. Under this assumption, $\text{TY}(G)$ is called a *Tambara-Yamagami theory*.

We call an anyon of charge q satisfying fusion rules of the form (5.2) a *Tambara-Yamagami* anyon, or ‘TY-anyon’ for short. Note that all anyons of charge $g \in G$ are abelian, and that $d_q = \sqrt{d}$ by (2.4b). Given a pair of TY-anyons, we can realise a qudit whose logical basis corresponds to their $d = 2^n$ possible fusion outcomes. If we wish to use TY-anyons to carry out (i) teleportation of a state with m basis states or (ii) m -ary superdense coding, then we take $\text{TY}(\mathbb{Z}_2^n)$ such that $n \geq \log_2 m$.

5.2. Braid-free qudit teleportation. Following the same arguments as in Section 3.3, the fusion state $|\varphi\rangle$ of $N \geq 2$ TY-anyons can encode $\lfloor \frac{N}{2} \rfloor$ qudits. Throughout the rest of this section, we take N to be even.⁴⁰ Suppose Alice wishes to teleport the fusion state $|\varphi\rangle$; this can be achieved without braiding, as illustrated in Figure 18.⁴¹ We summarise the procedure according to the three phases highlighted between the horizontal dashed lines.

- (1) Charlie has shared the halves of $N/2$ e-dits between Alice and Bob. Alice and Bob have agreed on a predefined bijection $f : G \rightarrow \mathbb{Z}_d$.⁴²
- (2) Alice fuses the rightmost of her N TY-anyons with the leftmost of those sent by Charlie, producing an anyon of charge $g_N \in G$ with probability $1/d$. She sends dit $f(g_N)$ to Bob,⁴³ and fuses g_N with a TY-anyon to the immediate left. This continues until the N^{th} fusion, where outcome g_1 is obtained and $f(g_1)$ is sent to Bob.
- (3) After Bob has received all transmissions from Alice, he performs a sequence of splittings (according to the received dits) and fusions as shown in Figure 18. This leaves Bob with N TY-anyons in fusion state $|\varphi\rangle$ (and an ancillary anyon of charge g_1 to the immediate left).

³⁸It is straightforward to check that $\text{TY}(G)$ is nilpotent with nilpotency class 2.

³⁹Any braiding admitted by a unitary fusion category will also be unitary [30].

⁴⁰Note that $V^{q^{\otimes(2p+1)}} \cong V^{q^{\otimes 2p}}$ for $p \geq 1$. That is, given an collection of N TY-anyons for N odd, we can discard one of the outermost anyons without affecting the encoded fusion state. For this reason, we take $N = 2p$.

⁴¹Conversely, we see from Figure 18 that if Alice and Bob share p e-dits, they can teleport (at most) the state of $2p + 1$ TY-anyons.

⁴²Recalling the calculation in Section 3.2.1, 1 e-dit is encoded in the fusion state of two pairs of TY-anyons here (where each pair encodes one of the two maximally entangled qudits).

⁴³Since $d = 2^n$, 1 dit can be sent in the form of n bits.

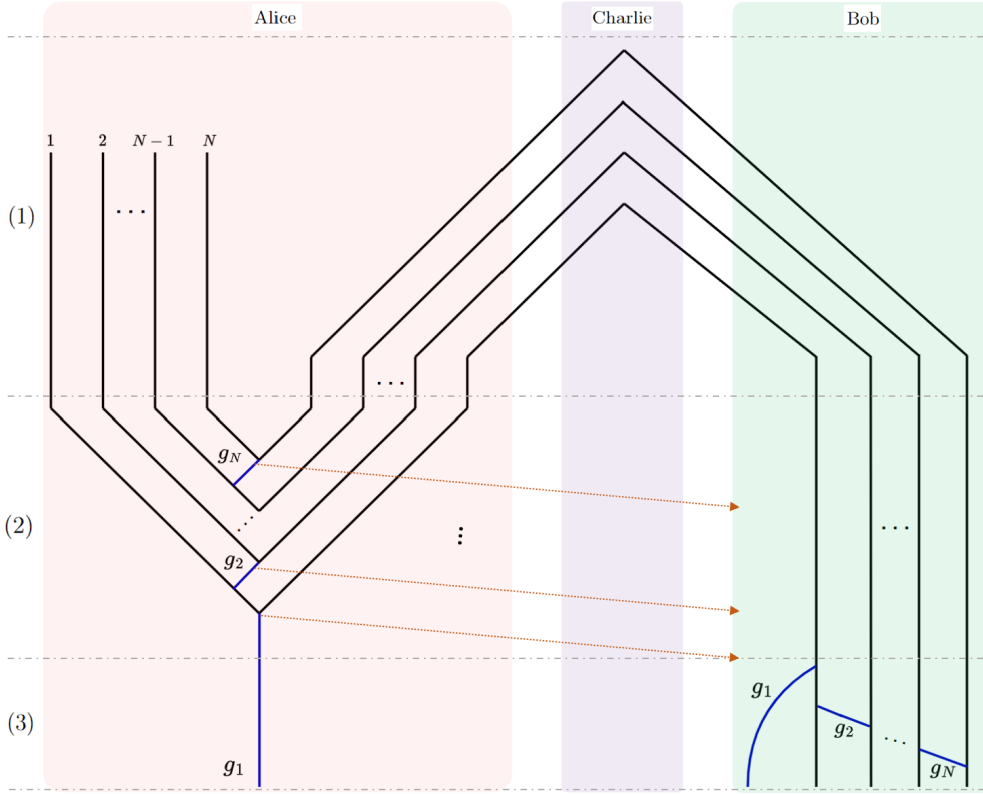


FIGURE 18. Braided teleportation. Solid black worldlines represent TY-anyons, and solid blue worldlines represent anyons of charge taking value in $G \cong \mathbb{Z}_2^n$. Dotted orange lines represent classical 1-bit transmissions from Alice to Bob. N is even.

Remark 5.5 (Bob's corrections). For any $j \in \{2, \dots, N\}$, Bob has the freedom to alternatively apply a correction via either of the processes (a)-(b) in (5.3); for $j = 1$, he may do so via (c).

$$(5.3) \quad \text{(a)} \quad \begin{array}{c} j-1 \quad j \\ | \quad | \\ | \quad | \\ \diagdown \quad / \\ | \quad | \\ | \quad | \end{array}, \quad \text{(b)} \quad \begin{array}{c} j-1 \quad j \\ | \quad | \\ | \quad | \\ \diagdown \quad / \\ | \quad | \\ | \quad | \end{array}, \quad \text{(c)} \quad \begin{array}{c} 1 \\ | \\ | \\ \diagdown \quad / \\ | \quad | \\ | \quad | \end{array}$$

Hence, the entire procedure may be carried out using only pair-creations (from the vacuum) and fusions (along with Alice's measurement of intermediate outcomes with charge in G).

The probability that Alice measures any charge $g \in G$ for a given fusion outcome g_j in Figure 18 is $\frac{1}{d}$. This follows from (5.4) and that $|[G_q^{qqq}]_{g0}| = \frac{1}{d_q}$ (by unitarity of L_0^{qq}).

$$(5.4) \quad \begin{array}{c} \diagdown \quad / \\ | \quad | \\ \diagdown \quad / \\ | \quad | \end{array} = \sum_g [G_q^{qqq}]_{g0} \begin{array}{c} \diagdown \quad / \\ | \quad | \\ | \quad | \end{array}$$

5.2.1. *Some useful results.* In the following, we relax the assumption that $G \cong \mathbb{Z}_2^n$ (i.e. that $\text{TY}(G)$ is braided), unless stated otherwise.

Lemma 5.6. *For each $g \in G$, we have*

$$\begin{array}{c} \diagdown \quad / \\ | \quad | \\ | \quad | \end{array} = L_q^{gq} \begin{array}{c} \diagdown \quad / \\ | \quad | \\ | \quad | \end{array}, \quad L_q^{gq} \in U(1)$$

Proof. Follows from the definition of L_{ab}^c in (2.13b) for $(a, b, c) = (g, q, q)$. □

Lemma 5.7. *In any gauge, it holds for each $h \in G$ that*

$$\left(\begin{array}{c} | \\ \hline h \\ \hline | \end{array} = \begin{array}{c} | \\ \hline h \\ \hline | \end{array} = \right) \left(\begin{array}{c} | \\ \hline h \\ \hline | \end{array} \right)$$

The proof of Lemma 5.7 presented below, relies on Lemmas 5.8-5.11. It will be useful to introduce shorthand notation for the following F -symbols.

$$(5.5) \quad [F_q^{qqq}]_{ij} =: f_{ij} \quad , \quad [G_q^{qqq}]_{ij} =: g_{ij}$$

Lemma 5.8. $|f_{ij}| = d_q^{-1}$ for all $i, j \in G$.

Proof. Solely within the scope of this proof, we will relabel Tambara-Yamagami charge q as x so as to avoid a clash of variables. Take pentagon equation (2.9) for $(a, b, c, d, e) = (x, x, \bar{j}, x, x)$, $(p, q) = (j, 0)$, $(r, s) = (x, i)$. That is,

$$[F_x^{xxx}]_{ij}[F_x^{j\bar{j}x}]_{x0} = [F_i^{x\bar{j}x}]_{xx}[F_x^{xxx}]_{i0}[F_0^{xx\bar{j}}]_{xj}$$

We note that $[F_x^{j\bar{j}x}]_{x0}$, $[F_i^{x\bar{j}x}]_{xx}$, $[F_0^{xx\bar{j}}]_{xj} \in \text{U}(1)$ since they act on 1-dimensional spaces. Thus, $f_{ij} = \omega \cdot f_{i0}$ where $\omega \in \text{U}(1)$. By unitarity of K_i^{xx} , $|f_{i0}| = d_x^{-1}$. The result follows. \square

Lemma 5.9. *For any $h \in G$,*

$$(i) \quad \begin{array}{c} \diagup \\ | \\ \hline h \\ \hline | \\ \diagdown \end{array} = (K_q^{qh})^* \left[\begin{array}{c} \text{---} \\ \text{---} \\ \text{---} \end{array} \right] + \sum_{j \neq 0} K_j^{qq} f_{jh} \begin{array}{c} \text{---} \\ | \\ \hline j \\ \hline | \\ \text{---} \end{array}$$

$$(ii) \quad \begin{array}{c} \diagup \\ | \\ \hline h \\ \hline | \\ \diagdown \end{array} = (L_q^{hq})^* \left[\begin{array}{c} \text{---} \\ \text{---} \\ \text{---} \end{array} \right] + \sum_{j \neq 0} L_j^{qq} g_{jh} \begin{array}{c} \text{---} \\ | \\ \hline j \\ \hline | \\ \text{---} \end{array}$$

Proof. We present the proof for (i); that of (ii) follows similarly.

$$\begin{array}{c} | \\ \hline h \\ \hline | \end{array} = b_0 \begin{array}{c} \text{---} \\ \text{---} \end{array} + \sum_{j \neq 0} b_j \begin{array}{c} \text{---} \\ | \\ \hline j \\ \hline | \\ \text{---} \end{array} \iff \begin{array}{c} | \\ \hline h \\ \hline | \end{array} = b_0 \begin{array}{c} \text{---} \\ \text{---} \end{array} + \sum_{j \neq 0} b_j \begin{array}{c} \text{---} \\ | \\ \hline j \\ \hline | \\ \text{---} \end{array}$$

$$\iff (K_q^{qh})^* \begin{array}{c} \text{---} \\ \text{---} \end{array} = \varkappa_q b_0 \begin{array}{c} \text{---} \\ \text{---} \end{array} + \sum_{j \neq 0} b_j (K_j^{qq})^* \begin{array}{c} \text{---} \\ | \\ \hline j \\ \hline | \\ \text{---} \end{array}$$

Then b_0, b_j are determined by comparing coefficients with change of basis transformation (2.7). \square

Lemma 5.10. *For $\text{TY}(G)$, there exists a choice of gauge \mathcal{G} such that*

$$(5.6) \quad f_{0j} = f_{j0} = \varkappa_q \sqrt{d_j/d_q} \quad , \quad j \in G$$

In this gauge,

- (i) $K_q^{qj} = L_q^{jq} = 1$ for all $j \in G$
- (ii) F_q^{qqq} is symmetric, i.e. $f_{ij} = f_{ji}$ for all $i, j \in G$
- (iii) $f_{ij}^* = f_{i\bar{j}} = f_{i\bar{j}}$ for all $i, j \in G$

Proof. This is an application of the results of [31]. \square

Consider the morphisms on the left-hand side of Lemma 5.9 (i)-(ii); we respectively denote these by linear operators $\mathcal{A}_h, \mathcal{B}_h$ on V^{qq} .

Lemma 5.11.

- (i) $\mathcal{A}_h, \mathcal{B}_h$ are physically gauge-invariant (but are not categorical invariants for $h \neq 0$).⁴⁴
(ii) In a gauge of form \mathcal{G} as in (5.6), we have

$$(5.7) \quad \begin{array}{c} \diagup \\ | \\ \diagdown \end{array} \begin{array}{c} h \\ | \\ h \end{array} \begin{array}{c} \diagdown \\ | \\ \diagup \end{array} = \frac{\sqrt{d_h}}{d_q} \begin{array}{c} \frown \\ | \\ \smile \end{array} + \varkappa_q \sum_{j \neq 0} f_{jh} \begin{array}{c} \frown \\ | \\ \smile \end{array} \begin{array}{c} j \\ | \\ j \end{array}, \quad \begin{array}{c} \diagdown \\ | \\ \diagup \end{array} \begin{array}{c} h \\ | \\ h \end{array} \begin{array}{c} \diagup \\ | \\ \diagdown \end{array} = \frac{\sqrt{d_h}}{d_q} \begin{array}{c} \smile \\ | \\ \frown \end{array} + \varkappa_q \sum_{j \neq 0} f_{jh}^* \begin{array}{c} \smile \\ | \\ \frown \end{array} \begin{array}{c} j \\ | \\ j \end{array}$$

- (iii) In a gauge of form \mathcal{G} as in (5.6), (a) operators $\mathcal{A}_h, \mathcal{B}_h$ are Hermitian and (b) $\mathcal{A}_h = \mathcal{B}_{\bar{h}}$.

Proof.

- (i) First, use (2.15) to substitute F -symbols for the leg-bending operators in Lemma 5.9. We then use (2.22a) to observe gauge transformations

$$(5.8) \quad \mathcal{A}_h \mapsto \mathcal{A}'_h = \alpha_h \mathcal{A}_h, \quad \mathcal{B}_h \mapsto \mathcal{B}'_h = \alpha_h^* \mathcal{B}_h, \quad \alpha_h = u_q^{qh}/u_q^{hq}$$

Although the operators are categorically gauge-dependent (save for $h = 0$ where $\mathcal{A}_0, \mathcal{B}_0$ are the identity operator), they are physically gauge-invariant (since the phase α_h is global).

- (ii) In this gauge, we have $K_j^{qq} = L_j^{qq} = \varkappa_q$. The result then follows by applying the results stated in Lemma 5.10 (specifically (5.6) and (i)-(ii)) to Lemma 5.9.
(iii) For convenience, we write the basis elements in (5.7) as e_g for $g \in G$. Then

$$\mathcal{A}_h = \frac{\sqrt{d_h}}{d_q} e_0 + \varkappa_q \sum_{j \neq 0} f_{jh} e_j \implies \mathcal{A}'_h = \frac{\sqrt{d_h}}{d_q} e_0 + \varkappa_q \sum_{j \neq 0} f_{jh}^* e_j$$

Then using Lemma 5.10(iii), we show the results.

- (a) $\sum_{j \neq 0} f_{jh}^* e_j = \sum_{j \neq 0} f_{\bar{j}h} e_{\bar{j}} = \sum_{j \neq 0} f_{jh} e_j$
(b) $\sum_{j \neq 0} f_{jh}^* e_{\bar{j}} = \sum_{j \neq 0} f_{j\bar{h}} e_{\bar{j}} = \sum_{j \neq 0} f_{j\bar{h}}^* e_j$

□

Proof of Lemma 5.7

We show that $\mathcal{A}_h = \mathcal{B}_h^{-1}$. Working in a gauge of form \mathcal{G} as in Lemma 5.10,

$$\left(\begin{array}{c} | \\ \diagdown \\ | \\ \diagup \\ | \end{array} \begin{array}{c} h \\ | \\ h \end{array} \begin{array}{c} \diagup \\ | \\ \diagdown \end{array} \right) = \left(\begin{array}{c} | \\ \diagdown \\ | \\ \diagup \\ | \end{array} \begin{array}{c} h \\ | \\ h \end{array} \begin{array}{c} \diagdown \\ | \\ \diagup \end{array} \right) = \frac{d_h}{d_q} \begin{array}{c} \frown \\ | \\ \smile \end{array} + \sum_{j \neq 0} |f_{jh}|^2 \frac{d_q}{\sqrt{d_j}} \begin{array}{c} \frown \\ | \\ \smile \end{array} \begin{array}{c} j \\ | \\ j \end{array} = \frac{1}{d_q} \sum_{g \in G} \begin{array}{c} \frown \\ | \\ \smile \end{array} \begin{array}{c} g \\ | \\ g \end{array} = \left(\begin{array}{c} | \\ \diagup \\ | \\ \diagdown \\ | \end{array} \begin{array}{c} h \\ | \\ h \end{array} \begin{array}{c} \diagdown \\ | \\ \diagup \end{array} \right)$$

In the second equality, we have composed the identities from (5.7) and used (the unnormalised form of) (2.3)(i). In the third equality, we have used Lemma 5.8 and that $d_g = 1$ for all $g \in G$. The final equality uses (the unnormalised form of) (2.3)(ii). Gauge-invariance follows from (5.8). □

Corollary 5.12. $\mathcal{A}_h, \mathcal{B}_h$ are unitary (for any choice of gauge) when $\text{TY}(G)$ admits a braiding.

Proof. We know that $\text{TY}(G)$ admits a braiding if and only if $G \cong \mathbb{Z}_2^n$. In this case, all elements of G are self-inverse. Then working in gauge \mathcal{G} from Lemma 5.10, it is clear from (5.7) that $\mathcal{A}_h = \mathcal{B}_h^\dagger$; but this holds true in any gauge by (5.8). The result follows since $\mathcal{A}_h = \mathcal{B}_h^{-1}$ (Lemma 5.7). □

Proof of Theorem 5.2

We show for either choice of fusion basis, and any choice of gauge, that $\{U_{g_1, g_2}\}_{g_1, g_2}$ coincides with the set of Pauli matrices (up to a global phase). Let us fix the same gauge as in Section 3.1. Since this gauge is of the same form as (5.6), we can apply Lemma 5.10(ii) to deduce that $\mathcal{A}_1 = \mathcal{B}_1 = Z$. By Lemma 5.10(i), we know that $\mathcal{A}_1, \mathcal{B}_1$ each coincide with Z (up to a global phase) in any gauge. Let $F := F_q^{qq}$. Using gauge transformation formula (2.22a), we see that for $\mathcal{E} \in \{\mathcal{A}_1, \mathcal{B}_1\}$, the matrices $F\mathcal{E}F^\dagger, F^\dagger\mathcal{E}F$ respectively coincide (up to a global phase) with $\mathcal{X}'_1, \mathcal{X}'_2$ in any gauge.

$$\mathcal{X}'_1 = \begin{pmatrix} 0 & \alpha^{-2} \\ 1 & 0 \end{pmatrix}, \quad \mathcal{X}'_2 = \begin{pmatrix} 0 & \beta^2 \\ 1 & 0 \end{pmatrix}, \quad \alpha = \frac{u_q^{q1} u_1^{qq}}{u_0^{qq}}, \quad \beta = \frac{u_0^{qq}}{u_1^{qq} u_q^{1q}}$$

⁴⁴By ‘physically gauge-invariant’, we mean gauge-invariant up to a $U(1)$ phase factor.

Since α, β are parametrised by gauge phases, they are not measurable and can be set to 1. That is, $\mathcal{X}'_1, \mathcal{X}'_2$ physically realise the Pauli-X matrix. Let \mathcal{C}_{g_j} denote the final element of the set of possible morphisms for coupon g_j in (5.1). \mathcal{C}_1 coincides with $\mathcal{A}_1, \mathcal{B}_1$ up to a global phase; see (5.10). \square

5.2.2. *A change of perspective.* Let us reconsider the issue of how Alice's measurements affect the state that she is teleporting. Although we analysed this relationship as part of the exposition in Sections 3.2.2 and 3.3, it will be instructive to reframe it in a way that appears 'natural' in the graphical calculus. To this end, we revisit phases (1)-(2) of the teleportation procedure for a single Ising qubit (from Figure 8). This coincides with phases (1)-(2) of Figure 18 for $N = 2$ and $G = \mathbb{Z}_2$.

$$(5.9) \quad \begin{array}{c} \text{Diagram 1} \\ \text{Diagram 2} \\ \text{Diagram 3} \end{array} = L_q^{iq} L_q^{jq} = L_q^{iq} L_q^{jq}$$

The first equality applies Lemma 5.6, and the second from straightening both zigzags (which incurs a factor of $\varkappa_q^2 = 1$). Let U_{ij} be the operator representation (on the state space V^{qq} of the Ising anyons) of the final two diagrams; then that of the first diagram is $L_q^{iq} L_q^{jq} U_{ij}$. Thus, the actions of these three processes on V^{qq} are physically equivalent.

Recall from Section 3.2 that if Alice measures both her fusion outcomes to be the vacuum, then Bob is in possession of her initial qubit without having to perform any corrections. Graphically, this is elucidated by the second equality of (5.9), where the worldlines are zigzags that can be straightened when both fusion outcomes are 0. Let $|\varphi\rangle$ denote the state of the Ising qubit that Alice wishes to teleport. Equation (5.9) offers a *change of perspective*, in telling us that Alice measuring fusion outcomes i, j is physically equivalent to having sent Bob a qubit $U_{ij}|\varphi\rangle$, where U_{ij} is graphically represented by the diagram within the dashed red boxes.

Let us fix the same gauge as in Section 3.1. Then $L_q^{iq} = L_q^{jq} = 1$, and by (3.8) we have that $U_{ij} = Z^j X^i$. Indeed, this can be understood in terms of the results of Section 5.2.1. The gauge we have fixed satisfies the form of gauge \mathcal{G} fixed in (5.6). Then by Lemma 5.11(ii), $\mathcal{B}_j = Z^j$. This leaves the question of how the 'stump' of charge i acts on the logical space, which we address in Figure 19.

$$(i) \quad \begin{array}{c} \text{Diagram 1} \\ \text{Diagram 2} \\ \text{Diagram 3} \end{array} = (K_q^{qi})^* \begin{array}{c} \text{Diagram 4} \end{array}, \quad (ii) \quad \begin{array}{c} \text{Diagram 5} \end{array}$$

FIGURE 19. The right two worldlines in (ii) correspond to the Ising anyons encoding Alice's qubit, while the leftmost is ancillary. By (i), we see that U_{ij} is effectively described by the action of the diagram in (ii) on $\bigoplus_k V_q^{qk} \otimes V_k^{qq}$. That is, the action of U_{ij} on Alice's qubit is equivalent to that of the operator $F_q^{qqq} \mathcal{B}_i G_q^{qqq} \mathcal{B}_j$ (which in the gauge fixed above is $X^i Z^j$).

Similarly, we can manipulate the diagram for phases (1)-(2) of the teleportation procedure for multiple Ising qubits (Figure 11) in the same way as we did for the single-qubit procedure in (5.9). We can then recover the state $|\varphi_{1,4}\rangle$ (as in (3.15), received by Bob before he applies corrections) using the results of Section 5.2.1.

5.2.3. *Proof of braidless teleportation procedure.* The process shown in Figure 18 corresponds to an operator $\mathcal{O} \in \text{End}(V^{q^{\otimes N}})$. In this section, we show that \mathcal{O} is equal (possibly up to a global phase) to the identity operator.

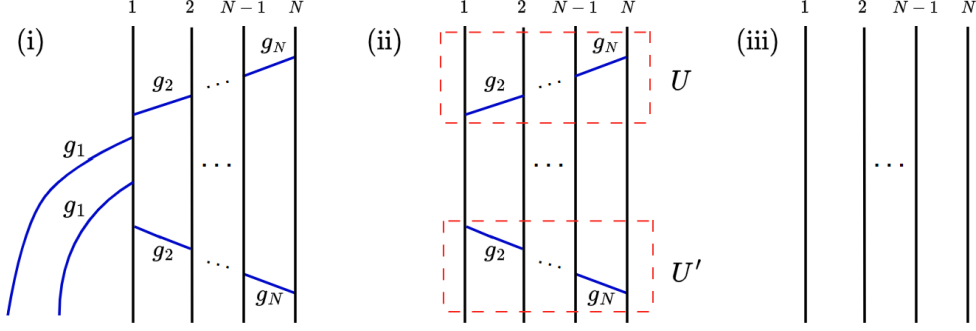


FIGURE 20. We will sequentially show that the process in Figure 18 is physically equivalent to those shown in (i)-(iii). Upon showing equivalence to identity operator (iii), we will have proved that the braided teleportation procedure works as claimed.

Applying Lemma 5.6 and straightening the N zigzags, we see that the process in Figure 18 is equivalent (up to a global phase of $\varkappa_q^N \prod_{j=1}^N L_q^{g_j q}$ which we can discard) to the one in Figure 20(i). Next, we consider the action of multiple ‘stumps’ (carrying charge valued in G) on the fusion state of the N TY-anyons.

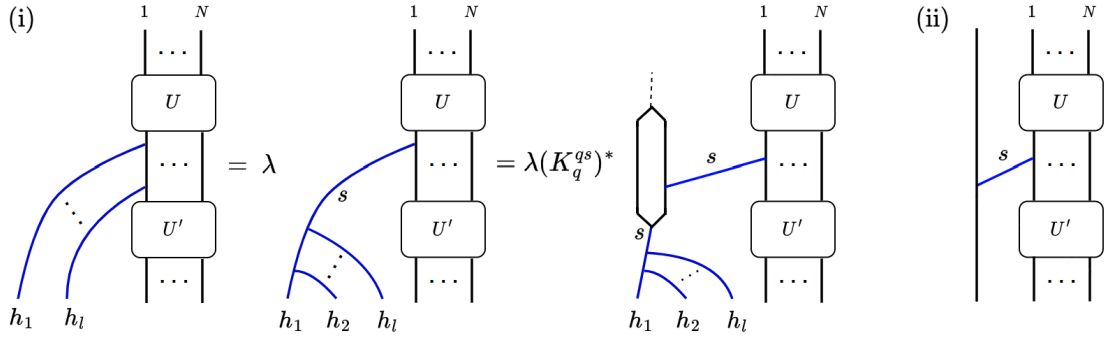


FIGURE 21. (i) Coupons $U, U' \in \text{End}(V^{q^{\otimes N}})$ represent some N -particle process. The first equality can be seen as a change of fusion basis on the 1-dimensional space $V_{h_1 \dots h_l}^q$ whence $\lambda \in U(1)$. We have $s = h_1 \dots h_l$. Then applying the identity from Figure 19(i) gives the second equality. (ii) The effective action of the $l \geq 2$ ‘stumps’ on the fusion state of N TY-anyons. When $s = 0$, this action is clearly trivial.

Let us consider the first equality of Figure 21(i) in the instance our system, Figure 20(i). We have that $l = 2$ and $h_1 = h_2 = g_1$ (whence $s = 0$ since $G \cong \mathbb{Z}_2^n$); also, $\lambda = [G_q^{g_1, g_1, q}]_{0q}^*$ and the stumps are effectively decoupled from the N TY-anyons. It follows that the action of the process in Figure 20(i) on the state of the N TY-anyons is physically equivalent to that of Figure 20(ii); linear operators U, U' are respectively identified with the processes enclosed within the dashed red boxes. By Corollary 5.12, we have that U is unitary and that $U' = U^\dagger$; thus, diagrams (ii) and (iii) of Figure 20 are equal.⁴⁵ This concludes the proof of Theorem 5.1.

All that remains is to justify the physical equivalence of substitutions (a)-(c) in Remark 5.3.

- (a) By Lemma 5.11(iii)(b), $\mathcal{A}_h = \mathcal{B}_h$ in gauge \mathcal{G} ;⁴⁶ thus, $\mathcal{B}_h^2 = \text{id}$ in this gauge. Then by (5.8), we have that $\mathcal{A}_h, \mathcal{B}_h$ coincide (up to a global phase factor) in any gauge, i.e. they act identically on the physical system. Similarly, \mathcal{B}_h^2 coincides (up to a global phase factor) with the identity operator in any gauge, whence its action on the physical system is trivial.

⁴⁵This equivalence is also shown by sequential application of Lemma 5.7 with respect to g_j for $j = 2, \dots, N$.

⁴⁶Then given gauge \mathcal{G} and TY(G) braided (i.e. $G \cong \mathbb{Z}_2^n$), F_q^{qqq} is real-symmetric with each element in $\pm 1/d_q$. The row and column corresponding to $0 \in G$ are given by (5.6). One can deduce that two distinct columns differ in 2^{n-1} entries (away from the 0-row), and that any non-0 column has an equal number of positive and negative elements.

(b) By (5.10), the substitution is equal (up to a global phase) to A_{g_j}, B_{g_j} .

$$(5.10) \quad \left| \begin{array}{c} g_j \\ \diagdown \quad \diagup \\ g_j \end{array} \right\rangle = K_q^{g_j q} \left| \begin{array}{c} g_j \\ \diagup \\ \diagdown \end{array} \right\rangle = L_q^{q g_j} \left| \begin{array}{c} g_j \\ \diagdown \\ \diagup \end{array} \right\rangle$$

(c) By (5.11), the substitution is equal (up to a global phase) to a g_1 -stump as in Figure 18.

$$(5.11) \quad \left| \begin{array}{c} g_1 \\ \diagdown \quad \diagup \\ g_1 \end{array} \right\rangle = K_q^{g_1 q} \left| \begin{array}{c} g_1 \\ \diagup \end{array} \right\rangle$$

5.3. Braid-free superdense coding of dits. Suppose Alice and Bob each possess half of a maximally entangled pair of TY-qudits. Alice wishes to encode a 2-dit string in her half and then send it to Bob. This can be achieved without braiding, as illustrated in Figure 22(i): we summarise the procedure according to the three phases highlighted between the horizontal dashed lines.

- (1) Charlie has shared the halves of 1 e-dit. between Alice and Bob. Alice and Bob have agreed on a predefined bijection $f : G \rightarrow \mathbb{Z}_d$.
- (2) Alice encodes dits $f(i), f(j)$ in her pair of TY-anyons, which she then transmits to Bob.
- (3) Bob receives Alice's qudit and performs two measurements in order to recover dits $f(i), f(j)$.

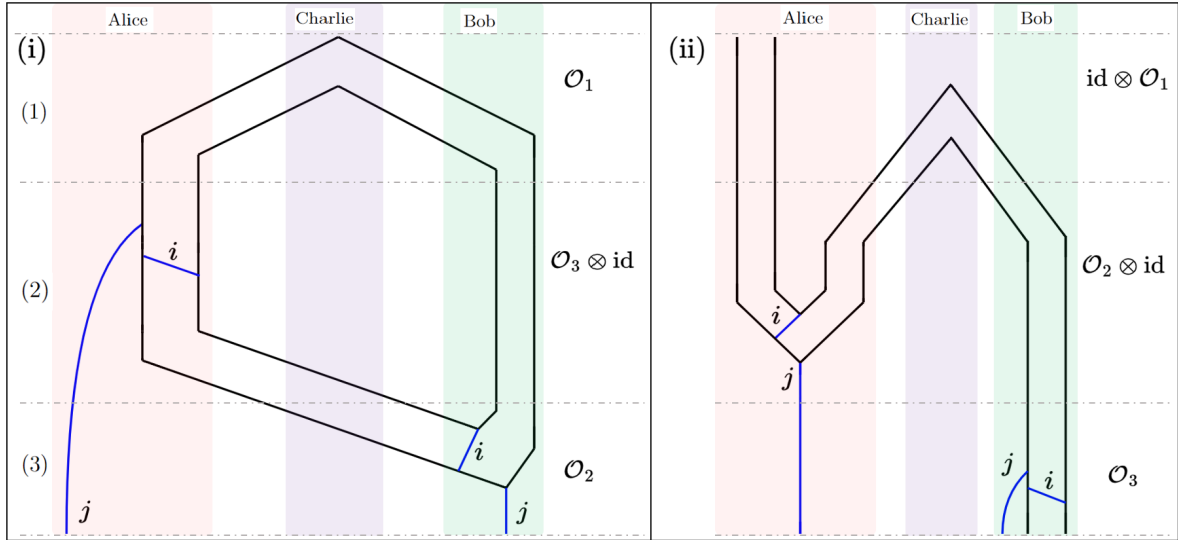


FIGURE 22. Solid black worldlines represent TY-anyons, and solid blue worldlines represent anyons of charge taking value in $G \cong \mathbb{Z}_2^n$. Diagrams demonstrate braidless realisations of (i) superdense encoding into 1 qudit, and (ii) teleportation of 1 qudit (i.e. the case $N = 2$ in Figure 18; classical transmissions not drawn).

Proof of Theorem 5.3

Applying orthogonality relation (2.3)(i) to the right-hand side of (5.12), we see that the only permissible labelling is $(x, y) = (i, j)$. Thus, the superdense coding procedure (as shown in Figure 22(i)) works as claimed.

$$(5.12) \quad \left| \begin{array}{c} i \\ \diagdown \quad \diagup \\ x \end{array} \right\rangle = L_q^{iq} L_q^{jq} (K_q^{jq})^* \left| \begin{array}{c} j \\ \diagdown \quad \diagup \\ y \end{array} \right\rangle$$

□

Remark 5.13.

- (i) Operations $\mathcal{O}_1, \mathcal{O}_2, \mathcal{O}_3$ are defined as in Remark 4.2 (with qudit replacing qubit). As highlighted for the braided case, there is a close relationship between (i) and (ii) in Figure 22; they are respectively described by $\mathcal{O}_2 \circ (\mathcal{O}_3 \otimes \text{id}) \circ \mathcal{O}_1$ and $\mathcal{O}_3 \circ (\mathcal{O}_2 \otimes \text{id}) \circ (\text{id} \otimes \mathcal{O}_1)$.
- (ii) The unitary operator \mathcal{O}_3 has alternative implementations as described in Remark 5.3. For example, in Figure 22(i), Alice can respectively pair-create charges i, j from the vacuum, and then perform fusions to complete the encoding.

REFERENCES

- [1] Moore, G. and Read, N (1991). "Nonabelions in the Fractional Quantum Hall Effect". *Nucl. Phys. B*, 360(2-3).
- [2] Nakamura, J., Liang, S., Gardner, G.C. and Manfra, M.J. (2020). "Direct Observation of Anyonic Braiding Statistics". *Nature Physics*, 16.
- [3] Bartolomei, H. et al. (2020). "Fractional Statistics in Anyon Collisions". *Science*, 368(6487).
- [4] Willett, R.L. et al. "Interference Measurements of Non-Abelian $e/4$ and Abelian $e/2$ Quasiparticle Braiding". *Physical Review X*, 13(1).
- [5] Zhang et al. "Retraction Note: Quantized Majorana Conductance". (Retraction). *Nature*, 591.
- [6] Frolov, S. "Quantum Computing's Reproducibility Crisis: Majorana Fermions". *Nature*, 592.
- [7] Wang, Z. "Reconstructing CFTs from TQFTs". *YouTUBE*, uploaded by Mathematical Picture Language, 7 October 2020. <https://www.youtube.com/watch?v=75M9rtsnmXA>
- [8] Huang et al. (2021). "Emulating Quantum Teleportation of a MZM Qubit". *Phys. Rev. Lett.*, 126(9).
- [9] Xu, C.Q. and Zhou, D.L. (2022). "Quantum Teleportation using Ising Anyons". *Physical Review A*, 106(1).
- [10] Bonesteel, N.E., Hormozi, L., Zikos, G. and Simon, S.H. (2007). "Quantum Computing with Non-Abelian Quasiparticles". *International Journal of Modern Physics B*, 21(8-9).
- [11] Bonderson, P., Shtengel, K. and Slingerland, J.K. (2008). "Interferometry of Non-Abelian Anyons". *Annals of Physics*, 323(11).
- [12] Siehler, J.A. (2000). "Braided Near-Group Categories". *Preprint*. <https://arxiv.org/abs/math/0011037>
- [13] Rowell, E.C. and Naidu, D. (2011). "A Finiteness Property for Braided Fusion Categories". *Algebras and Representation Theory*, 14.
- [14] Bravyi, S. (2006). "Universal Quantum Computation with the $\nu = 5/2$ Fractional Quantum Hall State". *Physical Review A*, 73.
- [15] Baraban, M., Bonesteel, N.E. and Simon, S.H. "Resources Required for Topological Quantum Factoring". *Physical Review A*, 81.
- [16] Das Sarma, S., Freedman, M. and Nayak, C. "Majorana Zero Modes and Topological Quantum Computation". *npj Quantum Information*, 1.
- [17] Narozniak, M., Dartiailh, M.C., Dowling, J.P., Shabani, J., and Byrnes, T. "Quantum Gates for MZMs in Topological Superconductors in One-Dimensional Geometry". *Physical Review B*, 103.
- [18] Abramsky, S. and Coecke, B. (2004). "A Categorical Semantics of Quantum Protocols". *Proceedings of the 19th Annual IEEE Symposium on Logic in Computer Science*.
- [19] Coecke, B. (2006). "Kindergarten Quantum Mechanics: Lecture Notes". *AIP Conference Proceedings*, 810(1).
- [20] Heunen, C. and Vicary, J. (2019). "Categories for Quantum Theory: an Introduction". *Oxford University Press*.
- [21] Simon, S.H. (2021). "Topological Quantum: Lecture Notes and Proto-Book". *In preparation*. Draft available at: <https://www-thphys.physics.ox.ac.uk/people/SteveSimon/>
- [22] Kitaev, A. (2006). "Anyons in an Exactly Solved Model and Beyond". *Annals of Physics*, 321(1).
- [23] Valera, S.J. (2021). "Fusion Structure from Exchange Symmetry in $(2+1)$ -Dimensions". *Annals of Physics*, 429.
- [24] Vafa, C. (1988). "Towards Classification of Conformal Theories". *Physics Letters B*, 206(3).
- [25] Wolf, R. (2020). "Microscopic Models for Fusion Categories". PhD thesis, *Leibniz Universität Hannover*.
- [26] Fuchs, J., Runkel, I. and Schweigert, C. (2002). "A Reason for Fusion Rules to Be Even". *Journal of Physics A: Mathematical and General*, 35(19).
- [27] Simon, S.H. and Slingerland, J.K. (2022). "Straightening Out the Frobenius-Schur Indicator". *Preprint*. <https://arxiv.org/abs/2208.14500>
- [28] Tambara, D. and Yamagami, S. (1998). "Tensor Categories with Fusion Rules of Self-Duality for Finite Abelian Groups". *Journal of Algebra*, 209(2).
- [29] Galindo, C., Hong, S.M. and Rowell, E.C. (2013). "Generalized and Quasi-Localizations of Braid Group Representations". *International Mathematics Research Notices*, 2013(3).
- [30] Galindo, C. (2014). "On Braided and Ribbon Unitary Fusion Categories". *Canad. Math. Bull.*, 57(3).
- [31] Poudel, A. and Valera, S.J. *Manuscript in preparation*.